T H E U N I V E R S I T Y O F A L B E R T A

RELEASE FORM

NAME OF AUTHOR ..... Martin G. Connors .....

TITLE OF THESIS ..... Pulsars and Aligned Rotators .....

DEGREE FOR WHICH THESIS WAS PRESENTED ..... M.Sc. .....

YEAR THIS DEGREE GRANTED ..... 1979 .....

THE UNIVERSITY OF ALBERTA

PULSARS AND ALIGNED ROTATORS

by

MARTIN G. CONNORS

A THESIS

SUBMITTED TO THE FACULTY OF GRADUATE STUDIES AND RESEARCH

IN PARTIAL FULFILMENT OF THE REQUIREMENTS FOR THE DEGREE

OF MASTER OF SCIENCE

DEPARTMENT OF PHYSICS

EDMONTON, ALBERTA

FALL, 1979

THE UNIVERSITY OF ALBERTA

FACULTY OF GRADUATE STUDIES AND RESEARCH

The undersigned certify that they have read, and recommend to the Faculty of Graduate Studies and Research, for acceptance, a thesis entitled "Pulsars and aligned rotators," submitted by Martin G. Connors in partial fulfilment of the requirements for the degree of Master of Science.

ABSTRACT

A review of basic pulsar observations, complete until early 1979, is presented, followed by the arguments leading to the identification of neutron stars as the seat of the pulsar phenomenon. The basic properties of neutron stars as deduced from the Tolman-Oppenheimer-Volkoff equation and current ideas of high-density equations of state follow. The structure of matter at the surface of a magnetized neutron star is presented in a clear and consistent manner, and a mechanism to prevent the ionization of free atoms on the surface is proposed. Due to high binding energies and this mechanism it is shown that the neutron star surface must be ion-retentive over most of the star. The equations governing inertia-free plasma around the neutron star are presented and the vacuum electric field is found. The plasma charge density for a force-free magnetosphere and its physical conditions are discussed. Possible departures from force-free conditions and effects of stellar charge and surface ion retention are noted, and the formation of polar gaps above an aligned rotator where $\bar{\omega}\cdot\bar{\mu} < 0$ and charge is swept from polar regions is shown to be caused by the ion retention, according to the Ruderman-Sutherland theory. The characteristics of discharges due to pair production are discussed. It is proposed that synchrotron radiation from the produced pairs, and annihilation radiation from ejected positrons, will be observed from pulsars when observational techniques permit. Radiation mechanisms, especially those due to pair production, are briefly discussed.

ACKNOWLEDGEMENTS

For her love, support, and tolerance of my late hours, as well as the more tangible conversion of my handwriting into a readable draft text, I thank my wife, Sherry.

Discussions with my supervisor Dr. Hube, and his inspection of the progressing thesis, are gratefully acknowledged.

That my fellow graduate students Dave Henty, Randy Kobes, Manu Paranjape, and John Whitehead, would enthusiastically discuss neutron stars while not expecting me to reciprocate by discussing field theory, is noteworthy. Special thanks goes to Bob Brooks, who originally suggested the subject of pulsars, and provided me with a term paper about aspects of force-free magnetospheres, and to John Whitehead, who critiqued the third chapter.

I am grateful to Diana Zaiffdeen for a very competent and attractive typing job, and to my mother who financed it.

Finally I thank Dr. Israel who arranged financial support to make it possible to finish this thesis over the past summer.

TABLE OF CONTENTS

LIST OF FIGURES

A PARTIAL LIST OF SYMBOLS

a Radius of a neutron star	c Speed of light
$\bar{A}$ Vector potential	d Pulsar distance
B_o Magnetic induction at pole of a neutron star	E Energy
B_q Magnetic induction forcing relativistic electron motion (natural quantum mechanical measure of magnetic field strength)	$\bar{E}$ Electric field
B_{12} Magnetic induction in units of 10^{12} G	G Gravitational constant
$\bar{B}$ Magnetic induction or field	h Magnetosphere gap height

h	Planck's constant (reduced)
H	Magnetic intensity
I	Moment of inertia
$\bar{j}$	Current density
m	Particle mass or electron mass
M	Mass
$M_\odot$	Solar mass
n	Braking Index
n_+	Number density (ions)
n_-	Number density (electrons)
P	Rotation period
$P_i(\cos\theta)$	i^{th} Legendre polynomial

q_s Stellar charge

r Radial distance from origin

$\bar{r}$ Position

r_p Polar cap radius

t Time

$\bar{v}$ Particle velocity

$\hat{z}$ Unit vector in z-direction

α Fine structure constant

α Spectral index

$\bar{\beta}$ Velocity in units of c

γ Lorentz factor

ε Charge on a neutron star in units $\omega B_0 a^3/c$

η Magnetic diffusivity

θ Colatitude

θ_m Colatitude from magnetic pole

$\bar{\mu}$ Magnetic dipole moment

ξ Pair conversion parameter

ρ Density

ρ_f Field line radius of curvature

ρ_ℓ Radius of light cylinder

σ Surface charge density

σ Conductivity

τ Characteristic age of a pulsar

Ψ Toroidal angle

Φ	Electrostatic potential	$\bar{\omega}$	Angular velocity
χ	Obliquity of $\bar{\mu}$ and $\bar{\omega}$	ω_c	Critical frequency
ω	Radiation frequency	ω_i	Ionic gyration frequency

ABBREVIATIONS

CRM	Corotating magnetosphere	SNR	Supernova remnant
GR	General Relativity	TOV	Tolman-Oppenheimer-Volkoff
SN	Supernova		

CHAPTER 1

BASIC PROPERTIES OF PULSARS - OBSERVATIONS AND MODELS

Pulsars have aroused a large amount of interest since their discovery twelve years ago (Hewish et al. 1968). As a result there exists an extensive set of detailed observations of them, backed by a bewildering array of papers on pulsar theories. Despite this huge amount of effort in both observation and explanation, no fully satisfactory theory or model has yet been made to explain the details of pulsar emission. Indeed there has been a tendency to construct models independently explaining single aspects of the phenomenon, with hopes that these narrower views are not contradictory.

In making pulsar models, one uses established physical theory, guided by observational constraints, to arrive at a consistent solution. This may in turn predict further properties, which, if observed, lend more weight to the model. Since present-day models are limited in detail, we should examine the general properties which must be explained if we wish to claim any understanding at all of the pulsar mechanism.

More detailed discussions of observations are presented in two recent books (Manchester and Taylor 1977; Smith 1977).

Pulses

Regular pulses of enhanced emission are the defining characteristic of pulsars. The emission is from objects which are starlike in angular size, both at optical frequencies (see e.g. Peterson et al.

1978), and in the radio region after allowance for interstellar scintillation (Smith 1977; Andrew et al. 1964; Coles and Kaufman 1977). These pulses have broadband spectra and for various pulsars are observed in spectral regions from radio to gamma-ray. The pulses are themselves composed of one or more subpulses which occur with irregular timing and intensity, but such that a time-averaged intensity profile of a large number of pulses maintains an extremely stable shape, although one unique to each pulsar. With higher time resolution, the subpulses of 5 of 8 pulsars so studied (Cordes 1975) showed micro-pulses on a time scale of hundreds of microseconds. Secular changes in this stable integrated profile have been seen only in the case of the single known binary radio pulsar (Taylor et al. 1978). The period of the integrated profile is extremely stable, to as much as one part in 10^{12} over several years. Periods ranging from .033 s to 4.308 s have been observed. First derivatives of the period range from $+10^{-18}ss^{-1}$ to $+10^{-12}ss^{-1}$ for radio pulsars, and are larger in magnitude but negative in sign for the X-ray (binary) pulsars. Abrupt period decreases known as "glitches" have been observed in those two pulsars considered to be the youngest, the Crab pulsar P0531+21, and the Vela pulsar P0833-45, and also in P1641-45 (Manchester 1979). Small "'glitches' in a loose sense" have been observed in nine other pulsars in very accurate pulse timing studies (Gullahorn and Rankin 1978b).

The glitches of the Vela pulsar, illustrated in Figure 1, have been four in number (the last in July 1978), each a period decrease of about 200 nanoseconds, a fractional change of 2×10^{-6} in period. Glitches of the other two pulsars have been a factor of 100 smaller, and in the Crab vary in size. The period derivative decreases during

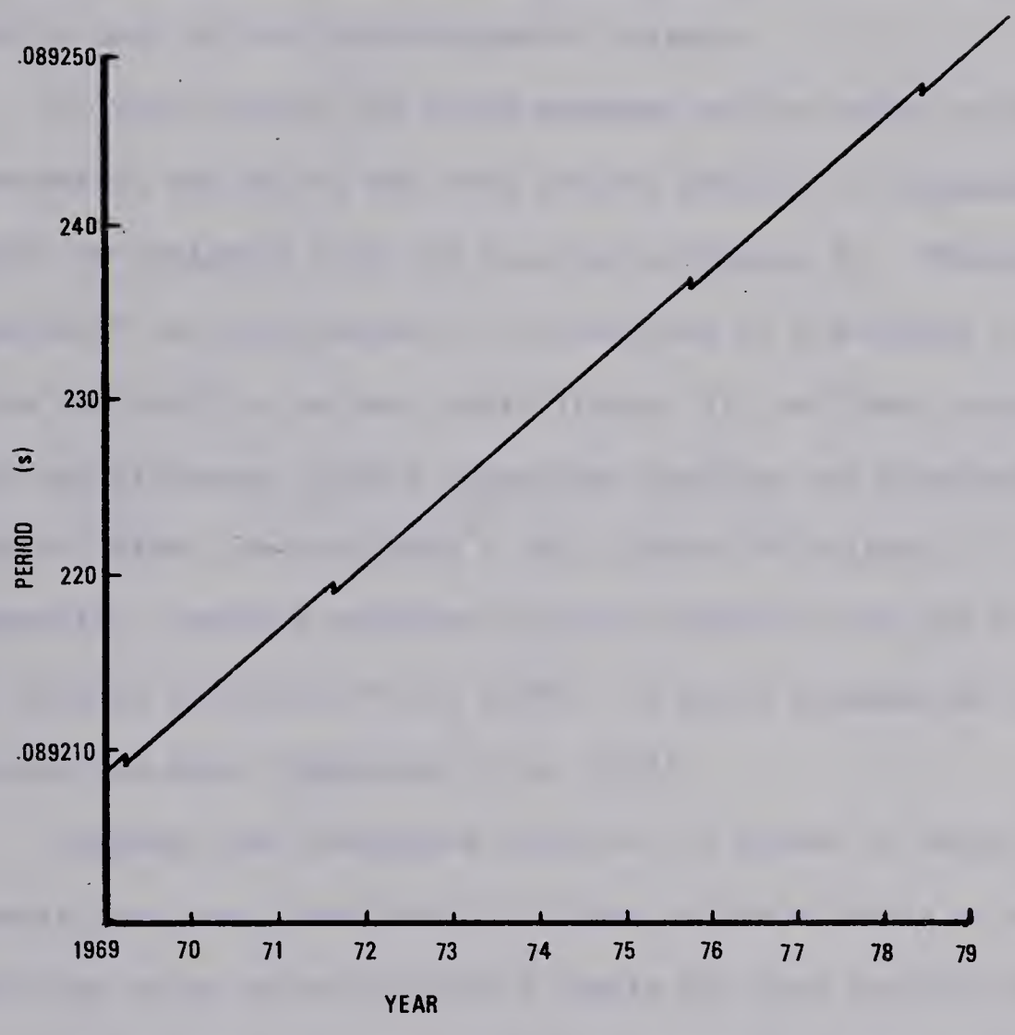

Figure 1. Glitches of the Vela Pulsar superposed on the continuously increasing period. (adapted from Manchester and Taylor 1977, p. 114, and Manchester 1979).

a glitch, the fractional change being measured in tenths of a percent. The period derivative returns to its pre-glitch value on a time scale of several days in the Crab pulsar, and of about a year in the Vela pulsar. Higher derivatives and irregular timing effects have been noted in most of the better-observed pulsars.

In most pulsars the radio emission occurs during only about 3 percent of the cycle, but some pulsars exhibit an "interpulse" roughly in antiphase with the main pulse (Figure 2). "Marching subpulses," the correlation of the position of a subpulse in one cycle to its position in the next cycle (Figure 3), and "mode changing," in which two different, stable integrated profiles are observed at different times, characterize a small number of pulsars. At optical frequencies, unpulsed emission has been observed from the Vela and Crab pulsars (Peterson et al. 1978). At radio frequencies the unpulsed component is small (Huguenin et al. 1971).

Although the integrated profiles are stable in shape, their intensity may vary considerably on time scales of hours or more, in some cases going below detectable levels for long periods of time.

The pulsed emission usually has very high linear polarization whose position angle changes monotonically across the integrated pulse. This polarization decreases with increasing frequency.

Pulsar emission peaks in the radio region and there the flux density S has a power law spectrum of form:

$$S(\nu) = S_o \nu^{\alpha} \qquad (1\text{-}1)$$

where $S_o = S(\nu_o)/\nu_o^{\alpha}$, ν is frequency, ν_o a reference frequency, and the index α typically about -1.5. (For a thermal source, the index α

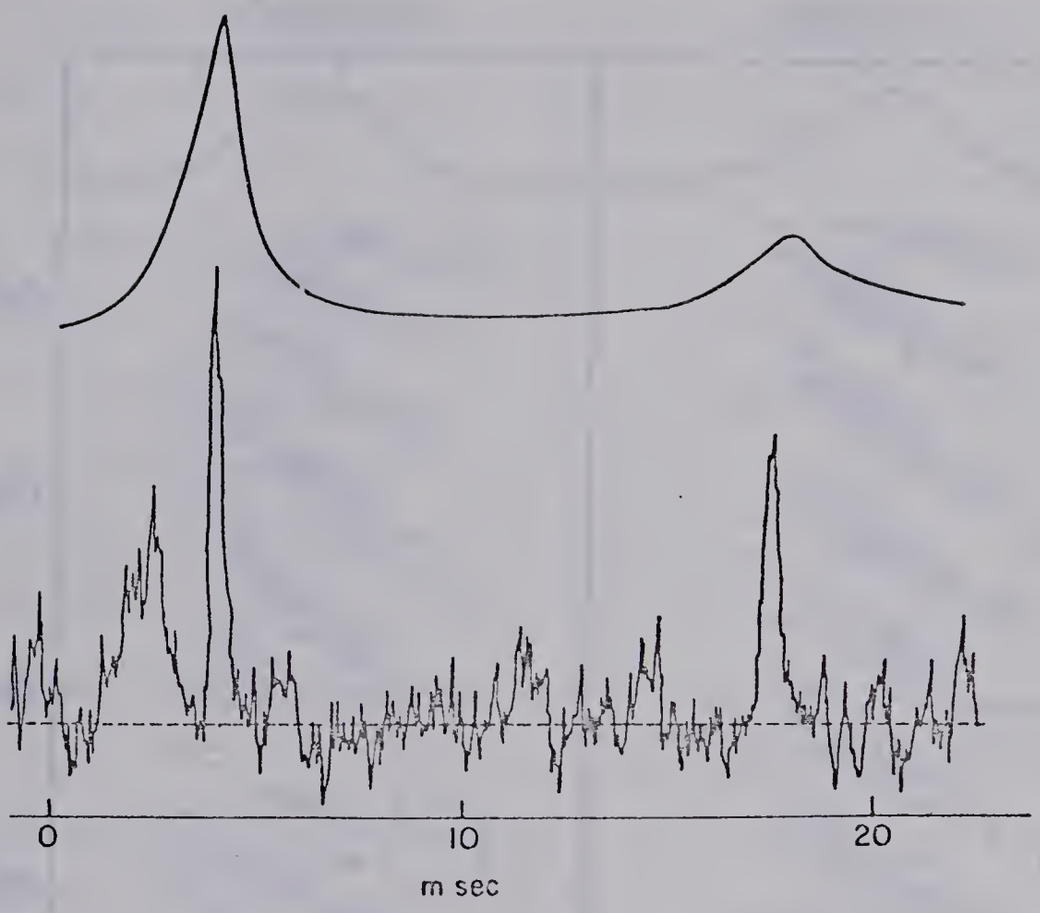

Figure 2. Pulse profiles of the Crab Pulsar P0531+21 at optical (above) and 430 MHz (below) frequencies. Very short timescale structures at radio frequency may be seen. (Drake 1970).

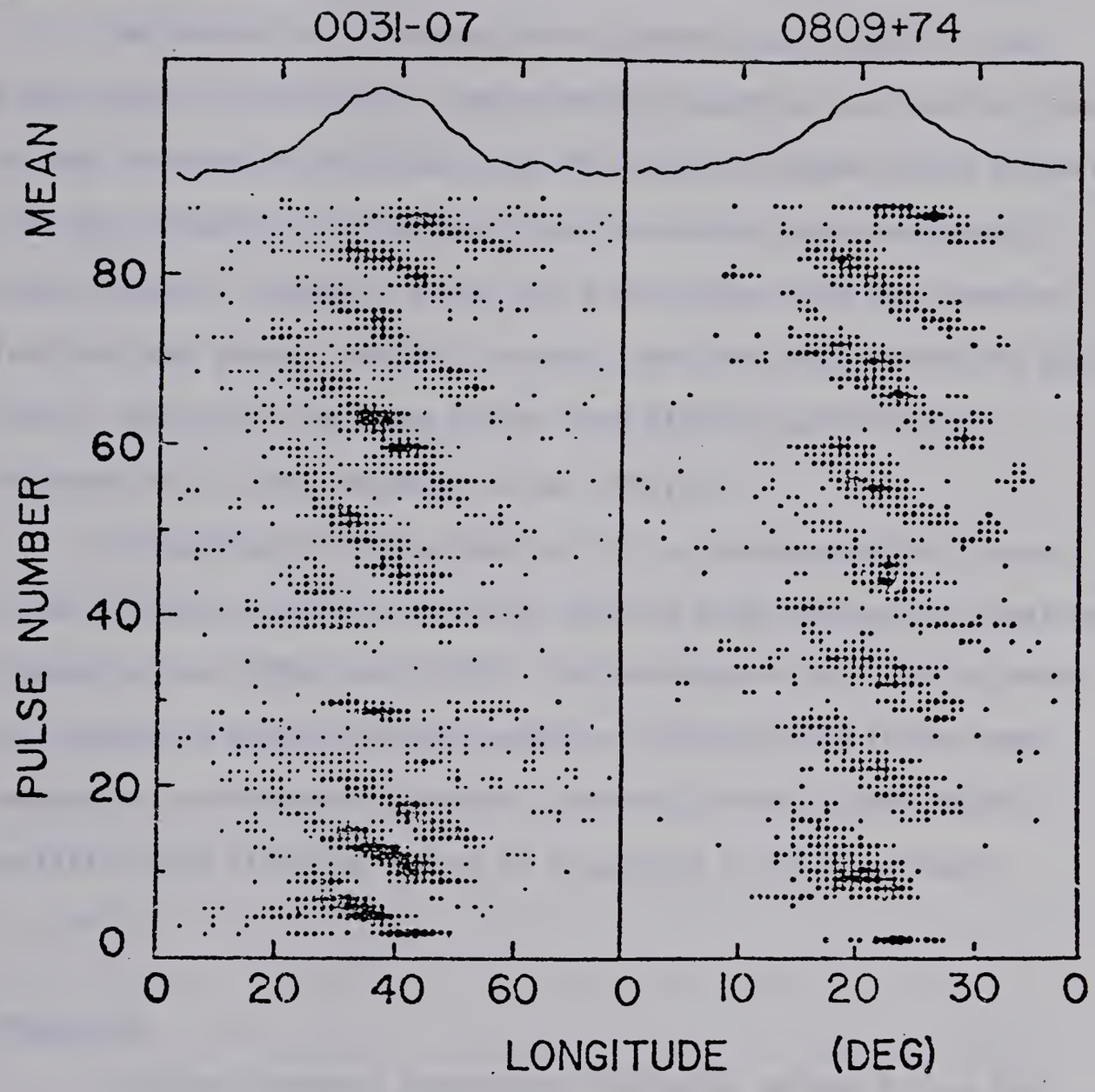

Figure 3. Drifting subpulses. The lines of horizontal dots represent individual pulses - the dot size reflects the intensity at a given longitude in the pulse. The integrated profiles are shown at the top. (Manchester 1979).

would have value +2.)

The binary X-ray pulsars, whose spectra peak sharply in the X-ray region, do not follow this power law spectrum, but the fact that at high frequencies, only the Crab, Vela and two longer-period pulsars have been observed, is consistent with this steep spectrum for all radio pulsars. (Optical, X-ray, and γ-ray pulses have been detected from the Crab pulsar, P0531+21, optical and γ-ray pulses from the Vela pulsar P0833-45, and γ-ray pulses from P1747-46 and P1818-04 (Ogleman et al. 1976; Buccheri et al. 1979).)

In the binary X-ray pulsar Her X-1, a strong emission line at 53 keV has been observed superposed upon an X-ray exponential spectrum (Trumper et al. 1977; Levi 1977). The intensity of the line is such that atomic or nuclear sources seem very unlikely, and it has been interpreted as electron cyclotron ("non-relativistic synchrotron") radiation from electrons moving in a magnetic field of strength 5×10^{12} G.

Luminosity

The high-frequency synchrotron radiation emitted by the Crab Nebula is steady in intensity for many years despite the fact that the electrons producing it have much shorter emitting lifetimes. The continuous injection of 10^{38} erg$\cdot$s^{-1} of energy carried by relativistic electrons from the Crab pulsar is the only plausible solution. The expansion of the nebula accelerates at a rate implying that a further 4×10^{38} erg$\cdot$s^{-1} are pumped into gas kinetic energy. The total luminosity of the pulsar must thus be at least 5×10^{38} erg$\cdot$s^{-1}.

The luminosity of pulsar emission cannot be directly measured because assuming isotropic emission (as is usually done with stars) does not seem justifiable. Thus, although flux can be measured, and the fact that the speed of radio waves in the interstellar medium is frequency-dependent allows distances to be assigned, the luminosity of a pulsar depends upon the model chosen and only in this sense is it "observable." Thus only the Crab Nebula and the possibility that high energy cosmic ray electrons are pulsar-produced (Ostriker 1972) allow luminosities to be determined. More data on pulsar luminosity, from sources other than the Crab Nebula, would be very desirable.

The Crab Nebula contains a widespread magnetic field of one milligauss according to the interpretation of its continuum radiation as synchrotron radiation from electrons. This nebular field is too large in magnitude and extent to be explained without invoking the pulsar as its source.

Of limited physical significance without a model, but useful statistically in estimating the degree of completeness in pulsar surveys, is the luminosity function of pulsars in the solar neighborhood. Defining the luminosity, L, as

$$L = S_{400} d^2 \qquad (1\text{-}2)$$

where S_{400} is the 400 MHz flux density (in Jy) and d the distance in parsecs, the z-integrated luminosity function per semidecade luminosity interval is (Manchester and Taylor 1977, p. 150):

$$\Phi(L) = 350 L^{-1.12} \text{ kpc}^{-2} \qquad (1\text{-}3)$$

Mechanical Properties

A study of the binary pulsar P1913+16 (Taylor et al. 1978) has revealed effects predicted by General Relativity (GR) which could, however, instead be explained as tidal effects in the pulsar or its companion. If these effects are indeed from GR, a very rigid structure must characterize the two objects.

A mass of 1.39 ± .15 $M_\odot$ for the pulsar and 1.44 ± .15 $M_\odot$ for the companion were also determined.

In an analysis of 5 binary X-ray pulsars whose companions could be observed optically (Rappaport and Joss 1977b), pulsar masses ranging from 0 to 4 $M_\odot$ in individual cases are not observationally excluded. However, a common mass of 1.2 to 1.8 $M_\odot$ would be consistent with observations of all of the systems.

Statistical Properties

As of late 1978, 321 pulsars had been observed, 241 of them in surveys specifically designed to provide a meaningfully uniform statistical sample (Manchester et al. 1978; Damashek and Taylor 1978). Sources for statistical data presently available are appended to this thesis.

The observed distribution of periods is shown in Figure 4, and since searches have covered fairly equally periods in the range .01 to 10 seconds, which is plotted, this is likely to represent the true distribution of pulsar periods. The distribution is apparently unimodal: the slight dip at P = 1 s, which in less complete data appeared to indicate bimodality (Manchester and Taylor 1977, pp. 152-153) no longer seems significant.

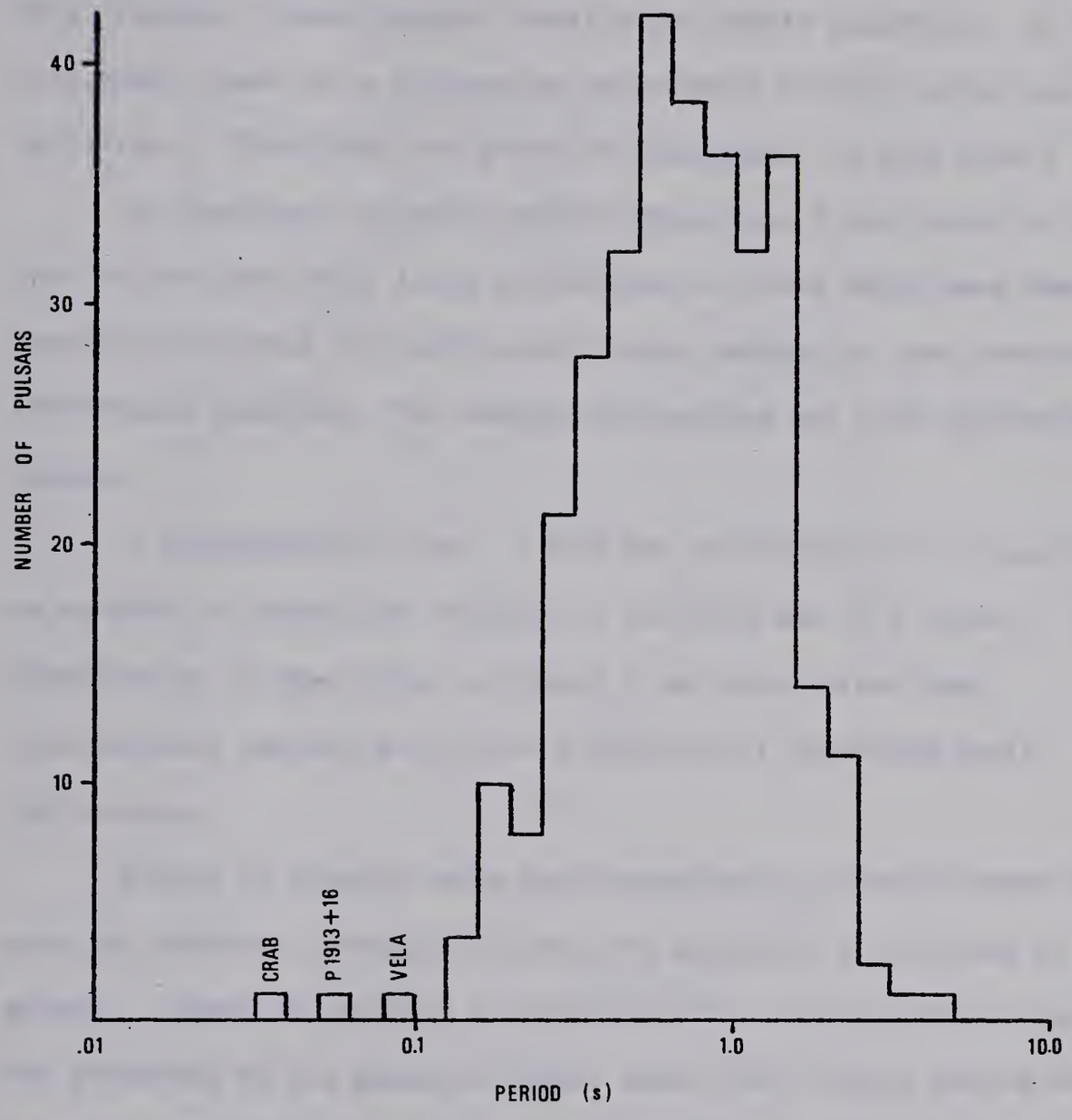

Figure 4. Distribution of periods among 321 radio pulsars. (Manchester 1979)

Period derivatives, when measured, are always positive for radio pulsars - their period steadily and slowly lengthens. As Figure 5 indicates, there is no pronounced correlation between period and derivative. (Note that the graph is logarithmic on both axes.)

An important selection effect which enters this graph is that only pulsars with very large derivatives or those which have been carefully observed for sufficiently large amounts of time have had their derivatives observed. The smaller derivatives are thus discriminated against.

A characteristic age $\tau = \frac{1}{2}P/\dot{P}$ may be defined and be expected to be an order of magnitude estimate of the true age of a pulsar. The distribution of ages shown in Figure 6 may have larger ages discriminated against due to the difficulty of observing small derivatives.

Figure 7a clearly shows the clustering of pulsars toward the galactic equator, proving that they are generally in the disk of our galaxy. Figure 7b, showing pulsars more than one kiloparsec from the Sun projected on the galactic plane, shows that surveys beyond about 5 kpc cannot be very complete, but that there is a real tendency for the pulsar density distribution to peak inside the galactic radius of the Sun. Figure 7, from Manchester (1979), is based on pulsar distances, d, calculated from dispersion measures (DM)

$$DM = \int_o^d n_e \, dl \qquad (1\text{-}4)$$

which can be measured due to the delay in pulse arrival times at frequencies ω_1 and ω_2, due to interstellar dispersion:

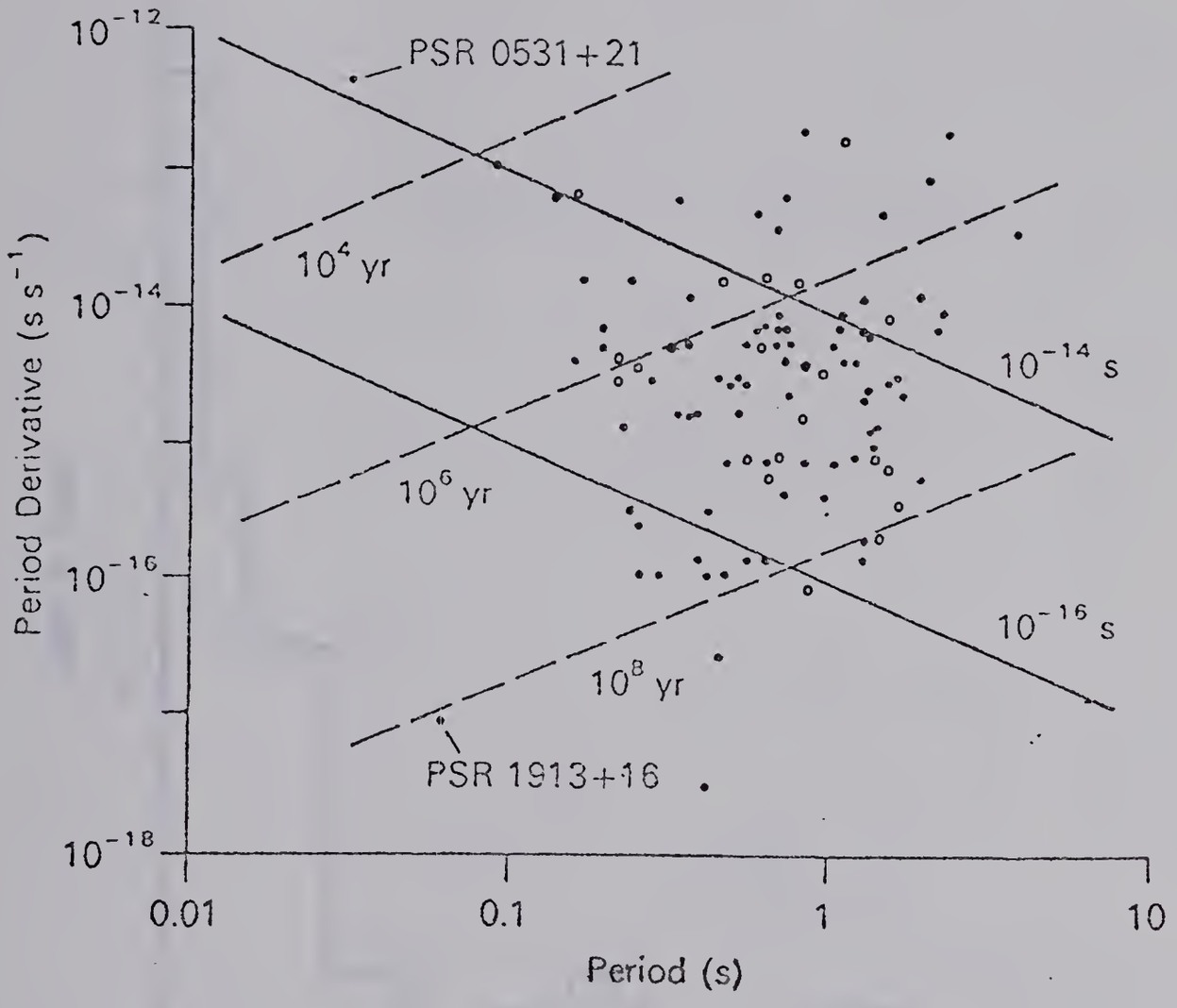

Figure 5. Period derivative versus period for 103 pulsars. Solid lines have constant $P\dot{P}$, dashed lines constant characteristic age. Solid dots are data from Manchester and Taylor 1977, p. 110, empty dots data from Gullahorn and Rankin 1978.

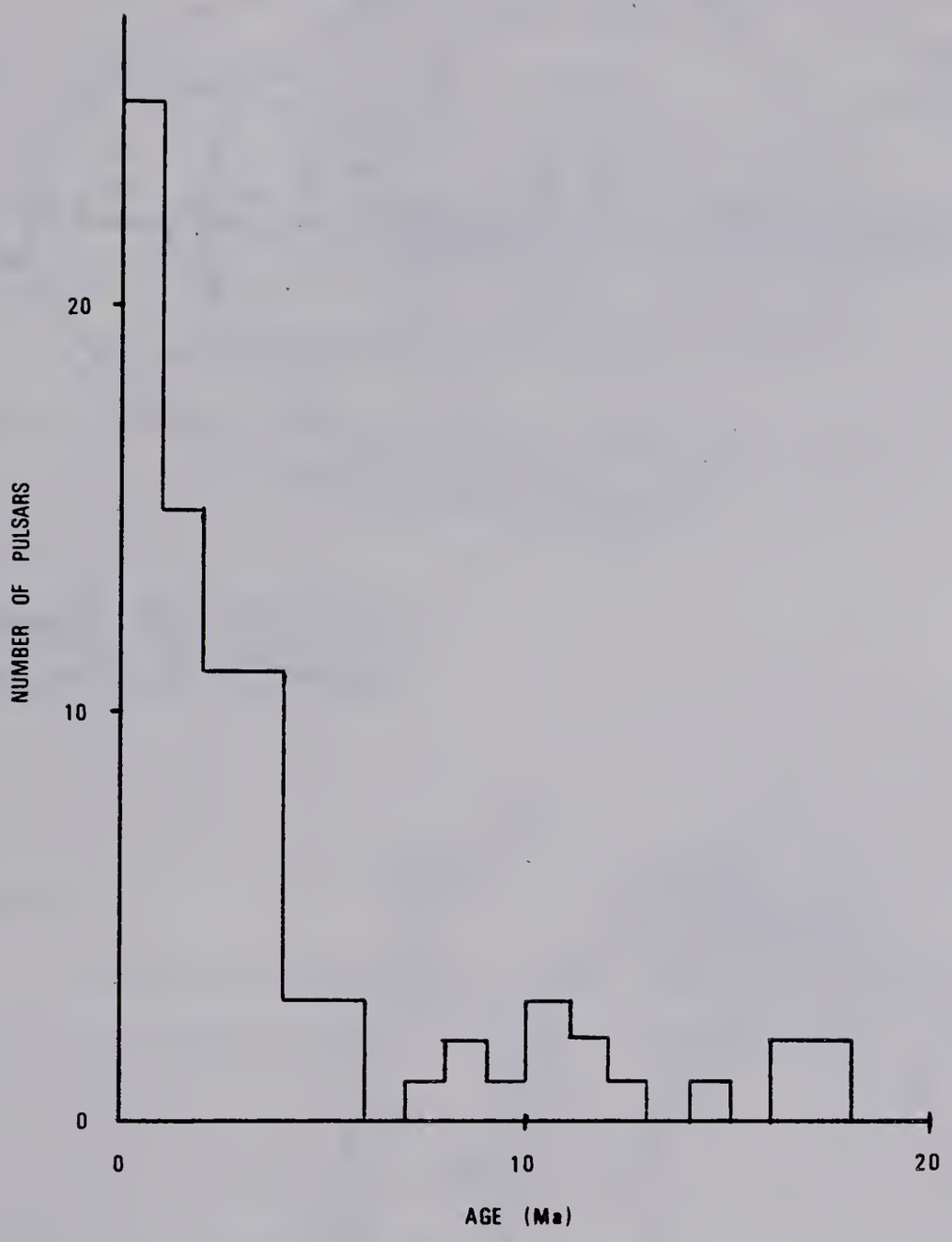

Figure 6. Distribution of 83 pulsar characteristic ages, τ, less than 2×10^7 a. (24 others have $\tau > 2 \times 10^7$ a). Data are from Manchester 1979, Gullahorn and Rankin 1978b.

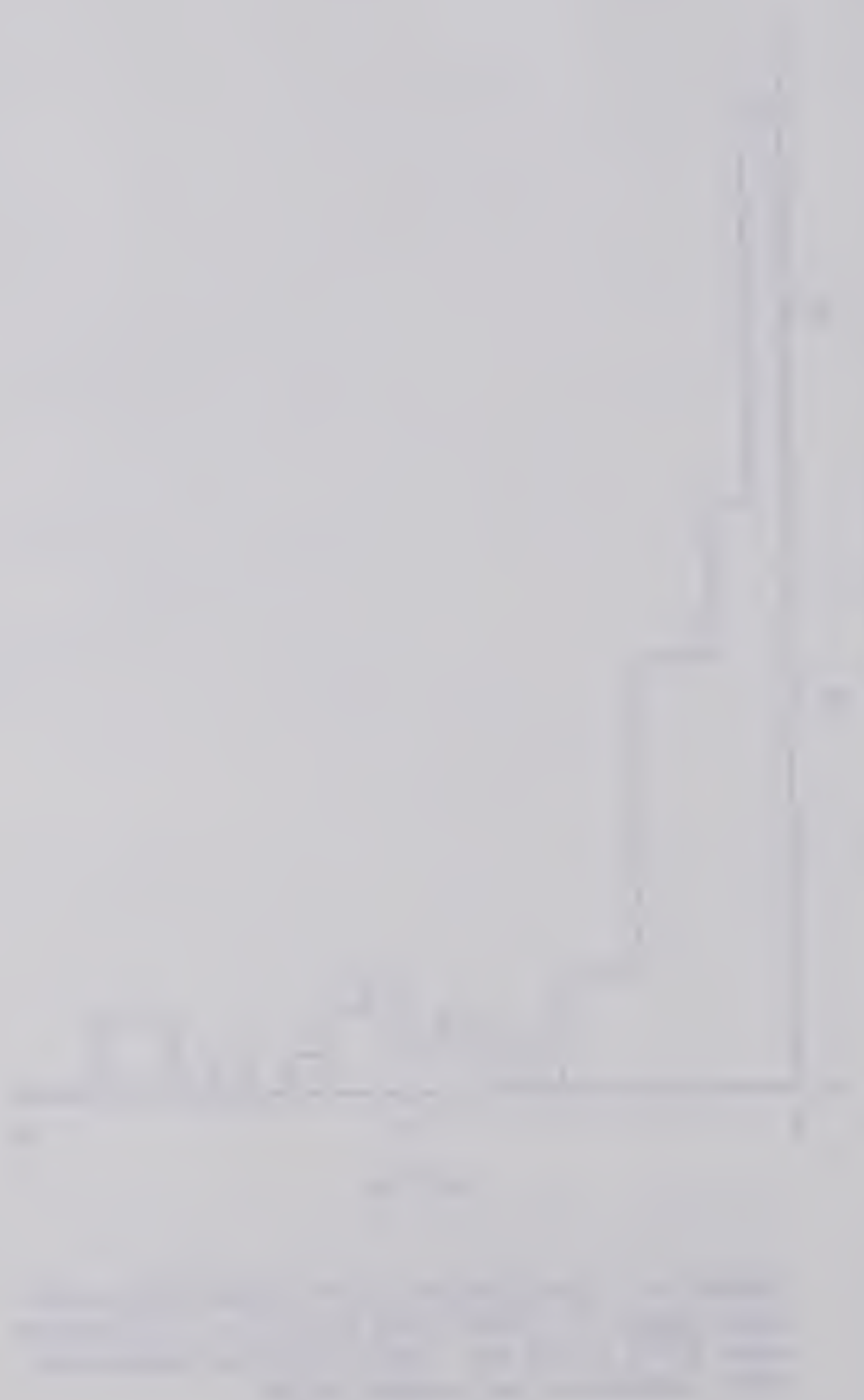

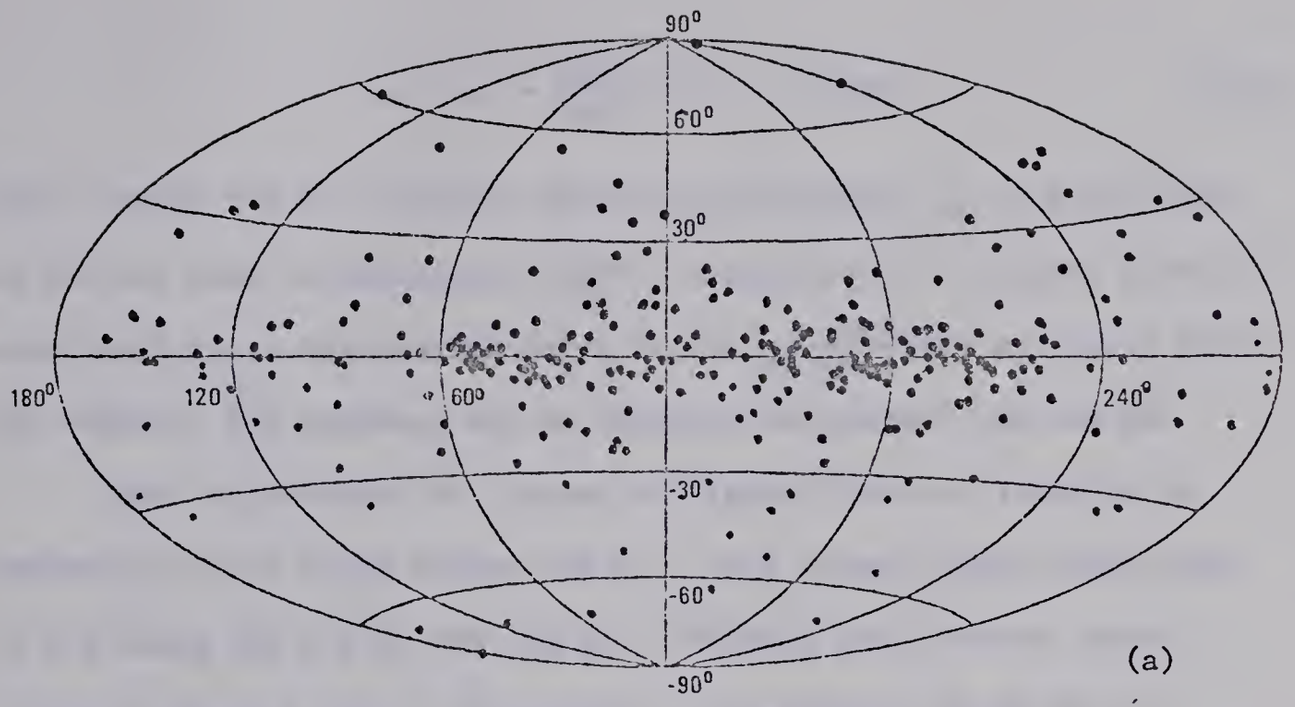

Figure 7. (a) Distribution in l and b of 321 pulsars.

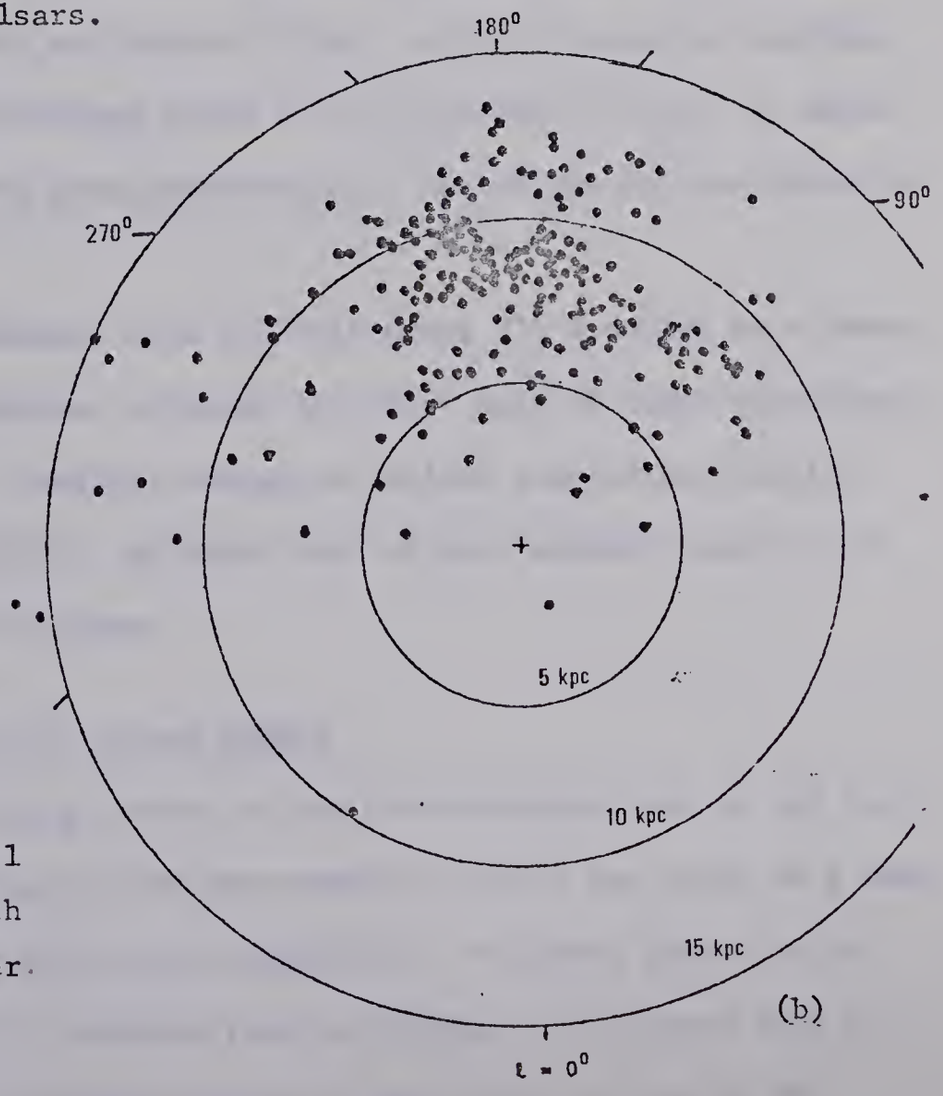

(b) Distribution in l and R of pulsars with d > 1 kpc. (Manchester 1979)

$$t_2 - t_1 = \frac{2\pi e^2}{mc}(\omega_2^{-2} - \omega_1^{-2})DM \qquad (1\text{-}5)$$

With a model for the electron density distribution, n_e (r,l,b), such as the one used in Manchester (1979), consisting of a uniform 0.025 cm^{-3} superposed on an exponential layer $0.015e^{\frac{-z\ kpc}{70\ kpc}}$ cm^{-3} and known local HII regions, the distance may be uniquely determined from the DM.

The distribution in z shown in Figure 8 can be fitted by an exponential with scale height 400 pc. This is much larger than that of O-B stars (80 pc) or SNR (60 pc). Pulsars are, however, high-velocity objects with an "unbiased" mean z-velocity of 60 km s^{-1} (Manchester 1979) based on measured proper motions (Manchester and Taylor 1977; Gullahorn and Rankin 1978a). At this velocity, the mean z of 300 pc would be reached (from z = 0) in about 5.5×10^6 a, which is of the order of the mean characteristic age of the pulsars shown in Figure 8.

Among radio pulsars only P1913+16 among 321 detected is a known member of a binary system, although for about half of these detections the data are not yet complete enough to exclude some being binaries (Manchester et al. 1978). At least half of the "normal" stars of our Galaxy are in binary systems.

Basic Characteristics of Pulsar Models

The most striking feature of the observational data is the very fact that pulsed emission from astronomical objects can occur on a very short time scale and with great regularity. The short period is so unique in astronomical contexts that an argument can be made that the reason that pulsars were not discovered until 1967 is that no one

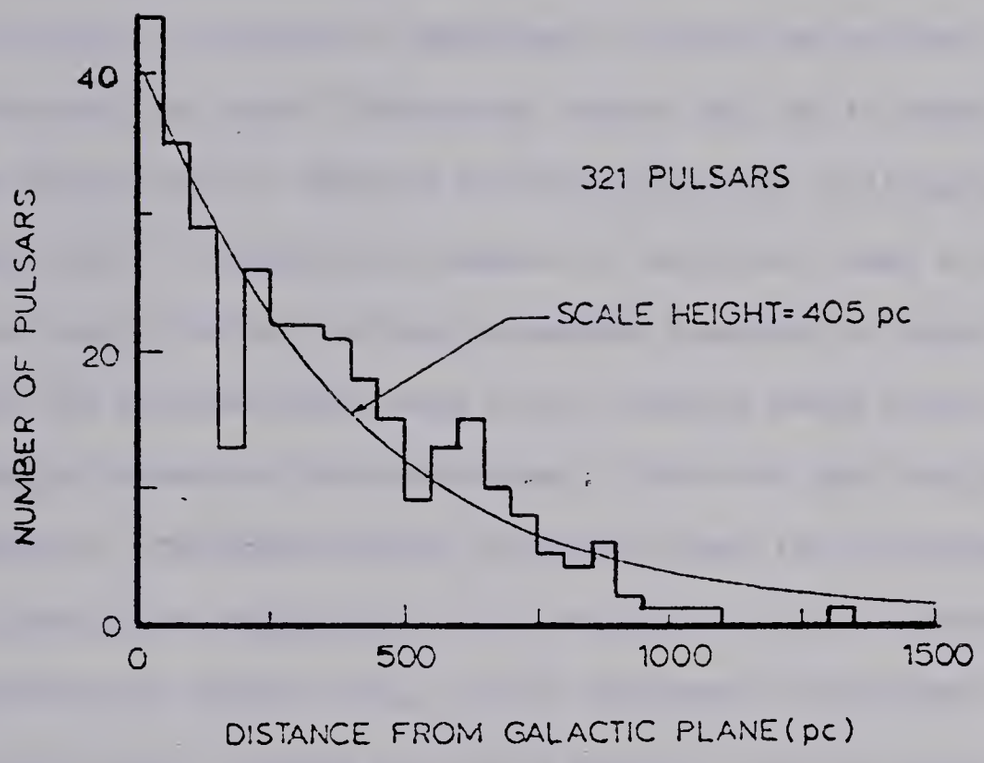

Figure 8. z-distribution of 321 pulsars.
(Manchester 1979)

looked. Indeed P0329+54 and the Crab pulsar were both recorded "before" pulsars were discovered but their unique signals not recognized (Smith 1977). After Jocelyn Bell's discovery in July 1967 of the signals of P1919+21 on recordings taken for the study of interstellar scintillation, the group at Cambridge, of which she was part, at first hypothesized that their "remarkable nature" was due to their generation by man (Hewish et al. 1968) or by "some silly lot of little green men" (Burnell 1977). However, the absence of parallax, code, or source's orbital Doppler shift, and the subsequent discovery of three further pulsars (by the Cambridge group in the cautious seven months between the initial discovery and publication), indicated that the phenomenon was natural. The pulse widths, of order 10 ms, led on the basis of light travel-time arguments to the conclusion that the sources would be of planetary or smaller size, and the discovery announcement (Hewish et al. 1968) itself proposed that white dwarfs or neutron stars generated the emission.

Pulsation of white dwarfs was initially favoured as the basic timing mechanism, pulsation periods as short as .07 s being possible for non-uniformly rotating white dwarfs (Durney et al. 1968). The discovery of the Crab and Vela pulsars, with considerably shorter periods, ruled out white dwarfs, and as neutron star pulsation periods are far too short, pulsation became disfavoured as a timing mechanism (Manchester and Taylor 1977). Theories invoking pulsation or explosive radial motion of only surface layers of white dwarfs or neutron stars (Hoyle and Narlikar 1968; Israel 1968a, b) also predicted periods of about one second.

Orbital motion about a neutron star could occur with periods down to about 1 ms and possibly cause the pulses by gravitational focusing (Saslaw et al. 1968) but gravitational radiation would cause the period to decrease, and the tidal forces acting on a satellite would require it to have unusual properties to remain intact (Smith 1977). The discovery of increasing periods for the Crab pulsar (Richards and Comella 1969), and subsequently for all others, led the orbital theory to disfavour.

The remaining mechanism involving condensed objects is that the rotation of a massive body acts as the timing standard, just as (until recently) on Earth. White dwarfs are stable against centrifugal breakup only for periods longer than one second (Ostriker 1968) and so were ruled out. Pacini (1967) had suggested that a rotating, magnetized neutron star could emit large amounts of energy in the form of low-frequency electromagnetic waves, and Gold (1968) was the first to propose such a star as the timing source in pulsars, and correctly predict that positive period derivatives should be seen due to the slowing of the rotation as energy radiated from the star.

By the middle of 1969 there was general agreement that Gold's model provided a basic timing mechanism with all of the needed properties. In the intervening ten years the problems of understanding the atmosphere of the neutron star and pulse production have "proven to be much more difficult than might have reasonably been anticipated" (Jackson 1976). The remaining chapters of this thesis address these problems.

For completeness, some post-1969 models, which are considered "non-standard" as opposed to the rotating neutron star hypothesis, will

be briefly discussed.

Similar in some respects to pulsational theories is the "bouncing-core theory" (Harrison 1970), in which the core of an object on the verge of gravitational collapse is unstable and does collapse periodically until a harder equation of state in the collapsed state, and changes in the metric around the object, halt and reverse the collapse. This model might allow periodicities of the right order, but the energy radiated through the non-collapsing crust (which is supported by radiation pressure) would likely be more like that of a blackbody than that observed in pulsars.

The solar cycle theory advanced by Apparao and Chitre (1970) attributes pulsar emission to activity similar to solar flares, associated with a neutron star magnetic cycle similar to that of the Sun but on a much shorter time scale. The precision of the periodicity and time derivatives are not convincingly explained by such a theory.

The mode-locked maser theory of Mertz (1974) explains pulse shapes and periods through a coherent mechanism in the resonant cavity formed by the surface of a white dwarf star and its hypothesized shell-like ionosphere. The supply of energy to such a resonant system for coherent emission is this theory's major difficulty.

The major gaps in these theories lend support to the neutron star hypothesis through "what-else-can-it-be" arguments. The ability of a rotating neutron star to explain timing observations, supply energy at appropriate rates, and explain certain radiation features, has led to the conviction that further work on it will eventually bear fruit, even though present models based on it are by no means fully satisfactory.

CHAPTER 2

STRUCTURE OF NEUTRON STARS

The aim of this brief discussion is to show that neutron stars could be expected to have masses and moments of inertia consistent with their being pulsars, and to discuss magnetic fields and boundary conditions which will be needed for the formulation of the pulsar mechanism as an electrodynamical problem.

Neutron Stars

Very soon after the discovery of the massive but electrically neutral neutron it was realised that a large number of neutrons could be held together gravitationally, with pressure support essentially due to the repulsive core of the nucleon potential, to form a stable condensed object. Oppenheimer and Volkoff in 1939 made the first neutron star model, and since the discovery of pulsars in 1967 and their "identification" as rotating neutron stars in 1968 (Gold 1968) much work has been done, to the point that most models agree on the general structure and differ only in detail, and thus may be considered satisfactory (Canuto 1977).

Within the framework of General Relativity (GR) the equation of hydrostatic equilibrium for a non-rotating spherically symmetric neutron star is the Tolman-Oppenheimer-Volkoff (TOV) equation

$$\frac{dP}{dr} = - \frac{G[\rho(r) + \frac{P(r)}{c^2}][m(r) + \frac{4\pi r^3 \rho(r)}{c^3}]}{r^2[1 - \frac{2Gm(r)}{rc^2}]} \qquad (2\text{-}1)$$

where $P(r)$ is the pressure, and $\rho(r)$ the density, at radius r,

$$m(r) = \int_0^r 4\pi\rho(r')r'^2 dr' \qquad (2\text{-}2)$$

being the mass interior to r.

Other gravitational theories than GR would cause differences from TOV solutions which vary from being very minor (Brans-Dicke theory) to non-negligible or even very large (Brecher and Caporaso 1977). However, such is the present status of GR that the use of the TOV equation has formed the core of recent neutron star theory (Canuto 1977). The consistency of neutron star and pulsar parameters with TOV predictions and with GR will be examined later in this chapter.

As is the case in non-relativistic stellar modelling, the use of an equation of state

$$P = P(\rho) \qquad (2\text{-}3)$$

and a boundary condition $P(R) = 0$ determines a unique total mass $M = m(R)$, and total radius R for a chosen central density ρ_c.

Five regions of distinctly different properties and equations of state may be identified in terms of density regimes (Lamb 1977):

1. The surface ($\rho < 10^6$ g cm^{-3}) where the effects of temperature and electromagnetic fields can be significant.
2. The outer crust (10^6 g cm$^{-3} < \rho < 4 \times 10^{11}$ g cm^{-3}); Here a solid lattice of nuclei is in a sea of degenerate relativistic electrons, as in white dwarf interiors. Iron (^{56}Fe), the most stable nucleus at low

pressure, will be the most abundant, until above 8×10^6 g cm^{-3} more neutron abundant nuclei predominate due to their inability to decay by releasing electrons into a full Fermi sea. At about 4×10^{11} g cm^{-3} is the "neutron drip point" where the nuclei are neutron saturated and free neutrons exist.

3. The inner crust (4×10^{11} g cm$^{-3} < \rho < 2 \times 10^{14}$ g cm^{-3}), below the drip point, contains a proportion of neutrons increasing rapidly with pressure until the lattice dissolves and a sea of neutrons, with only a few percent free electrons and protons, exists.
4. The neutron liquid exists above $\rho \simeq 2 \times 10^{14}$ g cm^{-3} until some possible critical density.
5. A core may exist, consisting of solid neutrons, hyperon or quark "soup," or pion condensate (Baym and Pethick 1975), for $\rho > 10^{15}$ g cm^{-3} (Manchester and Taylor 1977).

Integration of the TOV equation uses equations of state, $P = P(\rho)$, appropriate to these various regimes. The pressure in a neutron star is almost entirely due to zero-point energy, and thus any possible temperature dependence is ignored (Smith 1977, p. 36). Possible effects of temperature at the surface will be discussed later.

A recent review (Canuto 1977) of 10 TOV-based neutron star models showed that there is agreement among them in predicting masses of up to 2 $M_\odot$, moments of inertia in the range 10^{44}-10^{45} g cm^2, and radii of 8 to 12 km. These masses would be consistent with those of

pulsars discussed in Chapter 1.

From the understanding of the properties of matter in these five regions come predictions of further mechanical properties of neutron stars. The iron lattices at the surface and in the outer crust will be very rigid due to the large increases in Coulomb energy associated with any deformation from the lowest energy position. The neutrons in the inner crust and deeper are superfluid (Manchester and Taylor 1977), and are very weakly coupled to the crust.

The result of the rigid outer structure and superfluid interior is that "crustquakes" occur. As the neutron star loses rotational energy, its equilibrium shape changes. However, the rigidity of the outer crust does not allow it to deform continuously - instead stresses build up until a sudden deformation occurs, resulting in a decrease in (rotation-induced) oblateness and in moment of inertia. The conservation of angular momentum then forces a decrease in period of the crust. Due to the small coupling torque between crust and superfluid, which is proportional to their relative angular velocity, the torque slowing the crust is increased, and thus so is the rotation frequency derivative - the period derivative decreases, as is observed. As the interior and crust come to equilibrium, the torque vanishes and the period derivative returns to its previous value. This theory predicts the order of magnitude of the time interval between glitches in the Crab pulsar, but not for Vela. It has been hypothesized that the Vela glitches are due to "corequakes" in an hypothetical crystalline neutron core (Pines et al. 1974). Other "glitch" hypotheses are discussed by Manchester and Taylor (1977, pp. 190-197).

The electromagnetic properties of neutron stars are again fixed by the properties of matter throughout the star and its response to electromagnetic fields. These fields are presumed to be connected with the birth of the neutron star.

Formation of Neutron Stars

It is generally agreed that neutron stars are formed in supernova explosions. However, both observationally and theoretically the present evidence to back up this hypothesis is small. Only in the case of the Crab pulsar is the association with the Crab Nebula supernova remnant (SNR) unquestioned. The Vela pulsar is almost certainly associated with the Vela SNR, but only in a few other cases is there even a questionable association of pulsars and SNR's (Manchester and Taylor 1977, p. 167). A recent lunar occultation study of P0950+09 provided some evidence of a faint, radio-emitting SNR surrounding the pulsar (Gopal-Krishna 1978). There are several factors which could account for the failure to observe a significant SNR-pulsar correlation even if it does exist. Pulsar emission is believed to be beamed - in this case about 80% of pulsars would not be observable as their beam would not sweep Earth (assuming a random beaming direction and a beam width compatible with observation). This beaming and the impossibility of detecting very faint pulsars could explain why so few observed SNR's have had pulsars observed in them. SNR's generally expand and dissipate with age. Thus if the mean pulsar age is greater than one to two million years, any SNR which may have surrounded the young pulsar might by now have dissipated.

The estimated occurrence rate of supernovae in our Galaxy, based on observation and on stellar evolution theory, is between one per 20 years (based on SN in other galaxies) and one per one hundred years (radio SNR). This is in accord with the lowest estimated pulsar birthrates (Manchester 1979). It has been suggested (Cameron 1969) that non-supernova processes may also form neutron stars.

From the theoretical point of view, the late stages of evolution of the high-mass stars thought to be supernova progenitors are not well understood. Calculations in the 1960's showed that only extremely massive stars could avoid total disruption by a supernova explosion and so leave a remnant. This suggested that neutron stars would have to be formed otherwise, possibly in the slow contraction of a slightly over-massive white dwarf (Cameron 1969).

More recent calculations (Wheeler 1973; Bruen 1973) have indicated that for certain reasonable predetonation central density regimes (in the progenitor star), neutron stars should form in supernova explosions of degenerate stellar cores or of white dwarfs.

Massive close binary systems are expected to evolve very quickly to the stage where one of the stars becomes a SN. The material of the other star accretes onto the neutron star left by the explosion, and in this stage the system is an X-ray source (possibly an X-ray pulsar). As this star evolves, it also undergoes a SN explosion, and a pair of high velocity neutron stars will result, or a binary radio pulsar. This model explains observational statistics of the various guises of the binary system (close unevolved binary, binary X-ray source, pulsars) quite well and is the object of considerable study at present. See Manchester and Taylor (1977, p. 97) for

further details and references.

That high magnetic fields are expected in neutron stars is seen by considering that they are the result of the collapse of stellar material which is ionized and thus a good conductor. Thus the magnetic flux (through, say, the median plane of the star) is conserved, so that

$$\frac{B}{B_o} \propto \left(\frac{R_o}{R}\right)^2 \qquad (2\text{-}4)$$

where B_o and B are the magnetic fields at corresponding points in the star before and after collapse (here assumed to be merely a scaling radially), and R_o and R respectively the total radii before and after collapse.

A contraction factor of 10^5, which is that needed to "shrink" a star to the size of a neutron star, would result in a magnetic field amplification of 10^{10}. The fields of 500 to 3.4×10^4 G observed in magnetic stars could be "amplified" to the magnitude needed (10^{13} G) for current pulsar theories. It is also possible that magnetic fields are amplified in the cores of massive stars before a SN explosion (Angel 1978). These core fields would not be observable at the surface, and thus the relatively rare magnetic stars would not be the only possible neutron star progenitors. The fact that this mechanism would only occur in the most massive stars would explain the apparent paradox (Ruderman 1972) in the contraction hypothesis that only 3% of white dwarfs have intense magnetic fields. (A relatively small proportion of WD progenitors would be massive enough.) The observational evidence for a field of about 10^{12} G in the binary X-ray pulsar

Her X-1 has been cited.

Differential rotation in a collapsing star could cause the generation in the pulsar interior of a toroidal magnetic field of order 10^{15}-10^{17} G (Pacini 1973). The stresses produced by this field would cause a prolate distortion and polar wandering, and would stabilize the star against wobble from "glitches" and against alignment of magnetic and rotation axes if they are oblique (Goldreich, Pacini, and Rees 1971). This field would not be of direct significance at the surface.

A similar scaling occurs for the angular velocity, assuming a simple scaling of mass (this is very implausible but will provide a rough estimate). Amplification of angular velocity by about 10^{10} would decrease periods from 10^5 to 10^6 sec (main sequence stars' average) to 10^{-5} to 10^{-4} sec. We could thus expect neutron stars to have short periods, although other factors (gas ejection in SN, the density distribution differences of progenitor and neutron star, relativistic constraints) clearly enter a more quantitative discussion of this point.

CHAPTER 3

NEUTRON STAR SURFACES

The fact that quantum-mechanical effects at the surface of a neutron star could greatly influence magnetospheric structure was mentioned in the classic paper of Goldreich and Julian (1969). Since then these effects have been the subject of controversy. This chapter summarizes in a clear and consistent manner ideas originally put forth in a series of confusing papers by Ruderman, alone (1974, 1975), with Sutherland (1975), and with Chen and Sutherland (1974). The probable retention of ions in a pulsar surface, as predicted by the (incorrect) calculations of Chen, Ruderman, and Sutherland (1974), is discussed.

Effect of Magnetic Fields

In the interior region of neutron stars the effects of large magnetic fields are negligible compared with those of degeneracy (Canuto 1975b).

However, at the surface the fields which are inferred to exist (of order 10^{12}-10^{13} G), profoundly affect the properties of matter, in particular the opacity, conductivity, and emissivity of ions. The nature of the surface in turn determines the nature of the magnetosphere (Ruderman 1975).

The opacity due to the three major contributors - the free-free, bound-free, and Thomson scattering processes, for photons with $\bar{E}$ perpendicular to $\bar{H}$ - can be shown (Lodenquai et al. 1974) to be a factor $(\omega/\omega_H)^2$ smaller in the presence of a magnetic intensity H than

magnetic force is larger than the nuclear Coulomb force on the electrons, must be understood in order to specify the electrical properties.

The classical relativistic motion of a charged particle in a magnetic field of strength B is a helical orbit whose axis parallels the field, and whose radius is the Larmor radius;

$$R_L = \frac{\gamma v_\perp c m}{eB} = \frac{p_\perp c}{eB} \tag{3-1}$$

where $v_\perp$ is the component of the particle's velocity perpendicular to the field, and γmc^2 the particle's energy. R_L decreases with increasing B, and it is clear that when R_L is of the same order as the particle's de Broglie wavelength, the motion must be quantized. In similar fashion to the quantization procedure for the Bohr atom, it is required that the action in the plane of motion be quantized.

The old quantum theory applied to a spinless electron (Huang 1963) gives the quantization condition for the canonical momentum $\bar{p}$ (Landau and Lifshitz 1977, p. 171)

$$\oint \bar{p} \cdot d\bar{\ell} = (j + \tfrac{1}{2})h, \quad j = 0,1,\ldots \tag{3-2}$$

where the integral is around one orbit. The appropriate Hamiltonian is

$$H(\bar{p},\bar{r}) = \frac{1}{2m}(\bar{p} + \frac{e}{c}\bar{A})^2 \tag{3-3}$$

where e is the magnitude of the electron charge. The equation of motion

$$\frac{mv^2}{\rho} = \frac{ev}{c} B$$

in zero field, where $\omega << \omega_H$, and $\hbar\omega_H \equiv \hbar\frac{eH}{mc} = 10^4$-$10^5$ eV for a 10^{12}-10^{13} G surface field. An heuristic explanation of this effect for free-free scattering (Canuto 1975b) is that the electrons cannot interact normally with the $\bar{E}$ field when it is forcing them to move perpendicularly to magnetic field lines. This reduction of opacity speeds the cooling of neutron stars. However, slowdown of the internal superfluid neutrons is a source of thermal dissipation which will become important at a later stage (age 10^6 yr) of a pulsar's life to keep surface temperatures about 10^5-10^6 K (Manchester and Taylor 1977, p. 175). Young pulsars such as the Crab (10^3 a) and the Vela (10^4 a) could have temperatures in the 10^6-10^7 K range and thus emit unpulsed X-rays as black-body radiation (Tsuruta 1974). For the Crab, observations failing to detect such X-rays put an upper limit on the surface temperature of 4.7×10^6 K (Manchester and Taylor 1977, p. 175). The detection of unpulsed optical emission from both the Crab and Vela pulsars (Peterson et al. 1978), which is many orders of magnitude more intense than that expected from a neutron star emitting as a black body at $T = 2 \times 10^6$ K suggests a softening of higher-frequency radiation, as might occur in the case of X-rays emitted into plasma surrounding the pulsars. The detection of unpulsed X-rays from pulsars would be very important in fixing our ideas about their surface temperature.

The surface electrical properties are important in determining the structure of the neutron star magnetosphere since they determine its inner boundary conditions. The motions of the surface constituents in intense magnetic fields, and the properties of atoms when the

yields $$|\bar{v}| = v = \frac{e\rho}{mc} B \tag{3-4}$$

where ρ is the orbital radius, B the field, and m the electron mass, $\bar{v}$ being the electron velocity.

The canonical conjugate of the $\bar{p}$ in equation (3-2) is the position. Its derivative, the velocity $\bar{v}$, is thus given by Hamilton's equation:

$$\bar{v} = \nabla_p H = \frac{1}{m}(\bar{p} + \frac{e}{c} \bar{A}) \tag{3-5}$$

so that $$\bar{p} = m\bar{v} - \frac{e}{c} \bar{A} \tag{3-6}$$

and (3-2) becomes

$$\oint (m\bar{v} - \frac{e}{c} \bar{A}) \cdot d\ell = (j + \tfrac{1}{2})h \tag{3-7}$$

The first part integrates directly by symmetry to $2\pi\rho mv = 2\pi\rho^2 \frac{eB}{c}$, while the second has

$$\oint \bar{A} \cdot d\ell = \iint \nabla \times \bar{A} \cdot \hat{n} dS = \iint \bar{B} \cdot \hat{n} ds = \pi\rho^2 B \tag{3-8}$$

giving $$\pi\rho^2 \frac{eB}{c} = (j + \tfrac{1}{2})h$$

or $$\rho^2 = \frac{2c}{eB}(j + \tfrac{1}{2})\hbar \tag{3-9}$$

The energy is the numerical value of H in such a system, so

$$E = \frac{1}{2m}(\bar{p} + \frac{e}{c} \bar{A})^2 = \frac{m}{2}|\bar{v}|^2$$

$$= \frac{m}{2}(\frac{eB}{mc})^2 a^2$$

$$= \frac{e\hbar}{mc}(j + \tfrac{1}{2})B \qquad (3\text{-}10)$$

To describe real electrons the spin energy $-\bar{\mu}\cdot\bar{B}$ can now be added where

$$\bar{\mu} = -\frac{e}{mc}\frac{\hbar}{2}\hat{\sigma} \qquad (3\text{-}11)$$

and spin $\bar{\sigma}$ can be either parallel or antiparallel to $\bar{B}$. Thus the energy levels can be described as

$$E = \frac{e\hbar}{mc} nB = mc^2 n\frac{B}{B_q} \qquad n = 0,1,2... \qquad (3\text{-}12)$$

where B_q (usually denoted H_q) is $\frac{m^2c^3}{e\hbar} = 4.414 \times 10^{13}$ G.

Including a possible free motion along the magnetic field, with momentum p_z,

$$E = mc^2 n\frac{B}{B_q} + \frac{p_z^2}{2m} \qquad (3\text{-}13)$$

is the non-relativistic kinetic energy portion (obviously valid only when $nB << B_q$) of the exact Dirac equation energy set found by Rabi (1928)

$$E = mc^2\left[1 + \left(\frac{p_z}{mc}\right)^2 + 2n\frac{B}{B_q}\right]^{\frac{1}{2}} \qquad (3\text{-}14)$$

The level spacing in the non-relativistic approximation is mc^2B/B_q which is of order 10 to 100 keV in the fields of 10^{12} to 10^{13} G of a canonical magnetic neutron star. It is likely then that the vast majority of electrons are in the magnetic ground state, in a helix of

radius $\rho_o = (\frac{c\hbar}{eB})^{\frac{1}{2}} = 2.6 \times 10^{-10}/B_{12}^{\frac{1}{2}}$ cm, where B_{12} is in units of 10^{12} G. For fields of order 10^{12} G, this magnetic (Landau) radius is much smaller than the Bohr radius $a_o = 5 \times 10^{-9}$ cm, indicating that the role of a proton's Coulomb field, if present, would be that of a perturbation.

Since nuclei will be present at the surface, these Coulomb fields and the structure of atoms in very strong magnetic fields ($B \geq 10^{10}$ G) should be considered. A light atom takes the shape of a tube of the Landau radius with a length determined by Coulomb attraction. Treatment by perturbation methods (Landau and Lifshitz 1977, p. 460) or variationally (Ruderman 1974) gives a hydrogen ground-state energy (relative to motion in the lowest Landau level in the absence of a proton) of

$$E = \frac{me^4}{2\hbar^2} \ln \left(\frac{\hbar^3 B}{m^2 ce}\right) = -\frac{1}{2} \alpha^2 mc^2 \ln\left(\frac{B}{B_q} \frac{1}{\alpha^2}\right) \qquad (3\text{-}15)$$

where $\alpha = \frac{e^2}{\hbar c} \sim \frac{1}{137}$ is the fine structure constant. The quantity $\frac{1}{2}\alpha^2 mc^2$ is the binding energy of hydrogen in the absence of a magnetic field, 13.4 eV, so numerically

$$E \sim -13.4 \ln^2\left(19000 \frac{B}{B_q}\right) \text{eV}$$
$$\sim -700 \text{ to } -1200 \text{ eV for } B = 10^{12}\text{-}10^{13} \text{ G.} \qquad (3\text{-}16)$$

These values are reduced somewhat in more accurate calculations, but nevertheless serve to show that very large binding energies result from the "squeezing" of the atomic radius down to that of a Landau orbit, thus causing the electron to move deeper into the protonic Coulomb well than is normally possible. The length of the atomic "tube" is about

$a_o/\ell n(a_o/\rho_o)$ where a_o is the Bohr radius.

The consideration of multi-electron atoms is facilitated by solving the Schrödinger equation (Landau and Lifshitz 1977, p. 459) for wave functions associated with the Landau levels of a spinless electron, which can then be used in a Hartree calculation. The solutions are (Cohen et al. 1970)

$$\Psi_{n_\rho,m,p_z} = e^{-\frac{1}{2}\xi}\ \xi^{\frac{|m|}{2}}\omega(\xi)e^{im\phi}e^{ip_z z} \qquad (3\text{-}17)$$

where $\omega(\xi)$ is the normalized confluent hypergeometric function $F(-n_\rho, |m| + 1, \xi)$ (a Laguerre polynomial) and $\xi = \frac{eB}{2hc}\rho^2 = \frac{1}{2}\frac{\rho^2}{\rho_o^2}$, ρ being the radial coordinate. The positive integer n_ρ, corresponding to the n of equations (3-13) and (3-14), denotes the Landau level, and should be zero as we have seen, due to the large level spacing. The new quantum number m introduces degeneracy to the levels because for $n_\rho = 0$ the energy eigenvalues are not m-dependent. The motion along field lines is that of a free particle, $\exp[ip_z z]$. The introduction of a perturbing Coulomb field will remove the degeneracy in m, and also quantize the motion along the field lines. Calculations using a Hartree approximation have shown that the filling of orbitals in multi-electron atoms follows m rather than the quantum number associated with the z-motion (Chen et al. 1974). The Hartree wave-function for an atom of atomic number Z is (Cohen et al. 1970)

$$\Phi = \prod_{m=o}^{Z-1} e^{im\phi_m}R_m(\rho_m)f_m(z_m) \qquad (3\text{-}18)$$

where $R_m(\rho_m) = N_m\rho^m \exp(-\frac{\rho^2}{4\rho_o^2})$ (since $n_\rho = 0$ for all m), and $f_m(z_m)$ represents the z-dependence of the m^{th} particle's wave function. The

atom's energy was minimized by varying $f_m(Z_m)$ through a parameter α_m:

$$f_m(Z_m) = (\alpha_m)^{\frac{1}{2}} \exp(-\alpha_m |Z_m|)$$

In this way the total binding energies of atoms and their once-ionized states were found. The ionization energy, which then follows directly, is of order 135 eV for iron at 2.2×10^{12} G.

It is interesting to note that the radius where an electron of $n_\rho = 0$ and given m is most likely to be found is

$$\bar{\rho}_m = (2m + 1)^{\frac{1}{2}} \rho_o \qquad (3\text{-}19)$$

and is thus only slightly m-dependent. The electrons of a many-electron atom represented by (3-18) thus form a "hollow sheath" around a field line.

Such cylindrical atoms bind together (Kadomtsev and Kudryatsev 1971a) end-to-end, and form long chains consisting essentially of a sheath of electrons forming a Fermi gas in the "sheath," with the nuclei spaced along the field line centred within the sheath. Such chains in turn bind to one another to form a lattice when alternate ones are displaced by one-half the inter-nuclear spacing (Chen et al. 1974).

Emission Properties

For the mainly ^{56}Fe composition expected to be characteristic of the surface of neutron stars, in the magnetic field of 2×10^{12} G, the ions will have a cohesion energy of 4.1 keV (Flowers et al. 1977), and the electrons in the sheath will have a 750 eV Fermi energy (Chen et al. 1974). The incorrect prediction by Chen, Ruderman, and Sutherland (1974) that the cohesive energy of atoms to chains would be

14 keV at 2 x 10^{12} G led them to conclude that this binding into chains would alone prevent emission of ions from the surface. The lower cohesive forces now calculated, while implying that cohesion may not be entirely responsible for ion retention, do not imply that ions flow freely from the surface. The atoms which may be removed thermally from chains will form but a small percentage of the total number of atoms at the pulsar surface, since kT ≃ 10 eV << cohesive energy. Thus the Fermi energy of 750 eV, mentioned previously, will remain unchanged or nearly so. In any ionization, itself requiring 135 eV, the electron would have to acquire more than 750 eV to fill an allowed level above the Fermi sea. Due to this, free atoms on a pulsar surface cannot be ionized except by extremely energetic X-rays, which would probably have a very low interaction cross section with the outermost electrons of any atom present. This result would apply not only to iron but also to other atoms (such as helium (Michel 1975b)) which may be present in trace amounts (see Fawley et al. 1977). The fact that ionic field emission would be suppressed due to the fact that neutron star surfaces are protected against ion formation (from atoms), due to their high Fermi energy, has not been discussed in the literature.

It is worth noting that this protection mechanism is similar to that which allows neutrons to exist stably in the interior of a neutron star. Ruderman and Sutherland (1975) estimate that an applied field E such that $Z_c e \ell E$ is the order of the cohesive energy could separate ions of charge $Z_c e$, consisting of iron nuclei and several inner electrons. Even with the reduced cohesive energies recently calculated, a field of about 10^{11} V/cm would be required. While a field of this

order could be obtained for a pulsar rotating in vacuum (see Chapter 4), screening will occur in a realistic pulsar magnetosphere to prevent such high fields from developing. Ion retention thus will characterize pulsar surfaces.

Ruderman and Sutherland (1975) further argue that thermionic emission and sputtering due to the impact of relativistic electrons and positrons are negligible (however, see Chapter 4).

The emission of electrons depends very sensitively on the work function for the surface. This is not well determined but should be of the order of one keV. However electron emission is probably much easier than that of ions (Ruderman 1972a).

The conductivity of the atomic chains is essentially infinite parallel to the chain axes (field lines), since the electrons form a one-dimensional Fermi gas (Ruderman 1974). In the perpendicular direction it will be less (Ruderman 1971). Thus the surface conductivity is anisotropic.

Due to the formation of atomic chains bound to one another, the surface itself will end abruptly, and be more similar to that of a planet (or of "a not very smoothly shaved porcupine, with chains of Fe-atoms sticking out" (Borner 1973)) than that of a star.

The gravitational forces at the surface are very large, and for a neutron star of M solar masses and radius R_6 (in units of 10^6 cm) the gravitational potential energies of electrons and protons are -8×10^4 M/R_6 eV and -1.4×10^8 M/R_6 eV, respectively (Goldreich and Julian 1969). For $M \simeq 1$ and a typical $R_6 = 1$ these are about -.1 MeV and -100 MeV respectively.

To summarize, the surface of a rapidly rotating neutron star is subjected to the action of a very strong electric field sufficient to remove either electrons or ions. This particle outflow will guarantee that the star has a magnetosphere of charged particles, and the difference in ease of removal of electrons and ions has entered recent models in a very significant role (Ruderman 1975).

CHAPTER 4

PULSAR ELECTRODYNAMICS

The problem of the pulsar magnetosphere has not yet been "solved," in the sense that the behaviour of fields and particles in the vicinity of a rotating magnetic neutron star have not been detailed in a self-consistent manner. Most theories of pulse production consider the magnetic symmetry axis and that of rotation to be non-aligned - this departure from symmetry presumably being reflected in the highly anisotropic emission pattern thought to cause the pulses. However, such a problem is considered intractable, and most effort has gone into the simplified case of parallel or antiparallel magnetic and rotational axes. This special case removes both implicit time-dependence and axial asymmetry, and presumably the pulse, from pulsars. Despite these simplifications, even this problem has not been satisfactorily solved, partly because the magnetospheric plasma still retains many degrees of freedom, and also due to an incomplete understanding of the extreme physical conditions and of the boundary conditions involved.

The aligned rotator (magnetic and rotation axes parallel or antiparallel) will be considered first in some detail. The general features it possesses should be understood before we very briefly consider the more general non-aligned (oblique) rotator, to which they may, to an extent, also apply. Numerical models of non-aligned rotators are of some interest. After the basic structure of the magnetosphere is explained, in this chapter, the emission mechanisms which may account for the pulsed radiation will be considered, in the next.

In this chapter, unless otherwise specified, the neutron star itself will be considered as a rigidly rotating perfect conductor. While this approximation breaks down in some regions of the star, it will represent the overall steady-state situation accurately.

That electric fields play a major role in determining the magnetosperic structure was first suggested by Goldreich and Julian (1969), for the aligned rotator. The same basic argument holds for most of the surface of an oblique rotator (Cohen and Toton 1971).

The Vacuum Rotator

A perfect conductor, rotating in a magnetic field in a vacuum, acquires a charge distribution in its interior, which in turn produces an electric field. In a pulsar the force exerted by this field at the surface will remove charged particles to form a magnetosphere. The details of the vacuum aligned rotator problem, which follow, are as in Israel (1974). Since the conductivity is perfect, no charged particle within the star can feel a Lorentz force. At all internal points

$$\bar{E} + \frac{\bar{v}}{c} \times \bar{B} = 0 \qquad (4\text{-}1)$$

The particles rotate in the star and thus have velocity $\bar{v} = \bar{\omega} \times \bar{r}$. Fixing $\bar{\omega} = \omega\hat{z}$ and setting up non-rotating (see Webster and Whitten 1973) spherical coordinates centred on the star, and with the magnetic field symmetric about $\bar{\omega}$, the rotational symmetry means that $\frac{\partial}{\partial t} = \frac{\partial}{\partial \phi} = 0$. Immediately E_ϕ follows since $\bar{E} = -\nabla\Phi - \frac{\partial \bar{A}}{\partial t}$, where Φ is the scalar, and $\bar{A}$ the vector potential. The other components of $\bar{E}$ are most easily expressed by (4-1) where, now, $\bar{v} = \omega r \sin\theta \hat{\phi}$;

$$E_\theta = -(\frac{\bar{v}}{c} \times \bar{B})_\theta = -\frac{1}{c}\omega r\sin\theta\ Br$$

$$E_r = -(\frac{\bar{v}}{c} \times \bar{B})_r = \frac{1}{c}\omega r\sin\theta\ B_\theta \qquad (4\text{-}2)$$

Once the magnetic field components are specified, these relations, true within the star, allow the induced charge distribution to be calculated using

$$\rho = \frac{1}{4\pi}\nabla\cdot\bar{E} = -\frac{\omega}{2\pi c}\hat{z}\cdot\{\bar{B} - \frac{1}{2}\bar{r} \times (\nabla \times \bar{B})\} \qquad (4\text{-}3)$$

This induced charge distribution gives rise to an electric field externally as well as internally.

The external fields may be found by noting that in the vacuum surrounding the star Maxwell's equations are homogeneous and thus both the electric and magnetic fields are derivable from potentials. These potentials will be fixed by boundary conditions. In this case the tangential component E_θ of $\bar{E}$, and the normal component B_r of $\bar{B}$ are continuous at the surface (r = a). The electrostatic potential satisfies $\Phi \simeq O(\frac{1}{r^2})$ as $r \to \infty$, and solves $\nabla^2\Phi = 0$.

In the case of a dipole magnetic induction field of moment $\bar{\mu}$,

$$B_r = \frac{2\mu}{r^3}\cos\theta = B_o(\frac{a}{r})^3\cos\theta, \text{ and } B_\theta = \frac{\sin\theta}{r^3} = \frac{B_o}{2}(\frac{a}{r})^3\sin\theta \qquad (4\text{-}4)$$

where $B_o = B_r\ (r = a,\ \theta = 0) = \frac{2\mu}{a^3}$ is the magnetic induction (loosely, the magnetic field) at the pole. The boundary condition on the continuity of E_θ, from (4-2) and (4-4), is $E_\theta = -\frac{1}{a}(\frac{\partial\Phi}{\partial\theta})_{r=a}$ $= -\frac{B_o}{c}\omega(\frac{a^3\cos\theta\sin\theta}{r^2})_{r=a}$, which restricts the solution of Poisson's

equation for the electrostatic potential to

$$\Phi(r > a,\theta) = -\frac{1}{3}\frac{B_o \omega a^5}{c}\frac{P_2(\cos\theta)}{r^3} \qquad (4\text{-}5)$$

The field in (4-4) does not include some source of field (a point dipole), which would appear as a singularity at the origin (see e.g. Jackson 1975, pp. 138-141). Mestel (1971) notes that (4-4) would imply that the curl of the magnetic induction would be everywhere zero, which is unrealistic. Within the star he suggests that the field be regarded as uniformly $B_o\hat{z}$. The discontinuity in B_θ outside and inside would produce a surface current (Jackson 1975, pp. 19-21), in the direction $\hat{r} \times \hat{\theta} = \hat{\phi}$. Mestel's model also gives a different surface charge distribution,

$$\sigma = -\frac{\omega a B_o}{4\pi c}\left(\frac{5\cos^2\theta - 3}{2}\right) \qquad (4\text{-}6)$$

than will be found in (4-8) from Goldreich and Julian. In light of the anisotropy of the surface conductivity, as discussed in Chapter 3, it is worth noting that the Goldreich-Julian solution depends only on the E_θ boundary condition. With infinite conductivity in only the θ direction this boundary condition will not change despite the fact that the conductivity in r and ϕ may be very small.

However, in this case the continued existence of a current in the toroidal direction would be questionable. This problem, and that of an anisotropic oblique dipole rotator (discussed later), would be of great interest.

The external electric field from (4-5) has a radial component

$$E_r = -\frac{\partial \Phi}{\partial r} = -\frac{B_o \omega a^5}{cr^4}\frac{1}{2}(3\cos^2\theta - 1)$$

$$= -\frac{B_o \omega a}{2c}(3\cos^2\theta - 1) \quad (r = a) \tag{4-7}$$

while the radial component of the internal field is

$$E_r = \frac{B_o \omega a^3}{cr^2}\frac{1}{2}\sin^2\theta$$

$$= \frac{B_o \omega a}{2c}\sin^2\theta \quad (r = a) \tag{4-8}$$

The induced surface charge σ is $\frac{1}{4\pi}$ times the difference of (4-7) and (4-8), that is

$$\sigma = -\frac{B_o \omega a}{4\pi c}\cos^2\theta \tag{4-9}$$

More important, however, is the fact that there is a component of the electric field which can remove charged particles from the surface. In the strong magnetic fields near the surface the motion of charged particles is free only along the magnetic field lines. Thus the component of $\bar{E}$ along $\bar{B}$, of magnitude $\bar{E}\cdot\hat{B}$, is the source of energy increases of charged particles. ($\bar{E} \times \bar{B}$ drift velocities will be small since $|\bar{E}| << |\bar{B}|$ (Jackson 1975, p. 582), and are neglected.) $\bar{E}\cdot\bar{B}$, from (4-4) and the gradient of (4-5), is

$$\bar{E}\cdot\bar{B} = -\frac{B_o^2 \omega a^8}{cr^7}\cos^3\theta \tag{4-10a}$$

Inside, that $\bar{E}\cdot\bar{B} = 0$, which is implied by the Lorentz Force being zero, may be easily shown.

The problem of a perfectly conducting oblique rotator in vacuum was solved by Deutsch (1955). For a dipole field (Jackson 1978b;

(correction of his eq. 2.11)),

$$\bar{E}\cdot\bar{B} = -\frac{B_o^2\omega a^8}{cr^7}\frac{1}{4}\left[\left(\frac{r}{a}\right)^2(\cos\chi\cos\theta_m - \cos\theta - 4q_s\left(\frac{c}{\omega a^3 B_o}\right)\right.$$
$$\left. + 4\cos\theta\cos^2\theta_m - \cos\chi\cos\theta_m + \cos\theta\right] \qquad (4\text{-}10b)$$

where χ is the obliquity, θ the polar coordinate from the rotation axis, and θ_m the (time-dependent) polar coordinate from the magnetic axis. This result is valid only near the star (i.e., $r << \frac{c}{\omega}$), and a possible stellar charge q_s has been included. If $q_s = 0$, the difference from (4-10a) lies only in the time-dependent angular factor of magnitude about unity. Finding the effect of the anisotropic conductivity at the surface of a neutron star on Deutsch's vacuum solution would be an interesting problem in electrodynamics. Deutsch's general solution has surface currents which flow in both the poloidal (θ) and toroidal (ϕ) directions. At the neutron star surface only poloidal flow would be resistance-free. There would undoubtedly still be a similar value of $\bar{E}\cdot\bar{B}$, although the angular dependence would be different from that of equations (4-10).

The important result is that, depending on the surface conditions, positive or negative charged particles may be removed from a pulsar surface. A rotating, magnetized neutron star will <u>not</u> be surrounded by vacuum (Goldreich and Julian 1969), but rather by a magnetosphere, or magneto-electric atmosphere (Jackson 1978a), formed of charged particles extracted from the star.

The rate at which particles are pulled from the surface will obviously depend on their binding energy or work function. As discussed in Chapter 3 this differs for electrons and for ions and may be of large

magnitude (Ruderman 1975).

Another mechanism for "populating" the vicinity of the neutron star is the production of electron-positron pairs by γ-rays moving in the intense magnetic fields (Sturrock 1971; Erber 1966). The creation of pairs from the energy of the magnetic field alone is not possible (Chiu 1969).

However, before investigating the effects of a neutron star's plasma atmosphere, the radiation from an oblique magnetic dipole rotating in vacuum should be considered, as a rough guide to possible radiation mechanisms.

The power radiated by a non-constant magnetic dipole $\bar{\mu}$ is given by (Landau and Lifshitz 1962, p. 217):

$$\frac{dE}{dt} = -\frac{2}{3}\frac{\ddot{\mu}^2}{c^3}$$

Here $\ddot{\mu} = \omega^2\mu\sin\chi$, where the dipole makes an angle χ with the angular velocity $\bar{\omega}$. The rotating frame value of μ, $\frac{B_o a^3}{2}$, will be about the same in the non-rotating system which we are using due to the fact that $a\omega << c$, so that the power radiated will be

$$\frac{dE}{dt} = -\frac{1}{6}\frac{\omega^4 a^6 B_o{}^2 \sin^2\chi}{c^3} \qquad (4\text{-}11)$$

However, for a rotating body losing energy, $\frac{dE}{dt} = I\omega\dot{\omega}$, where I is the moment of inertia.

Equating these expressions for energy loss will give the expected rate of change of rotation frequency for a magnetic dipole associated with a spinning body:

$$\dot{\omega} = -\frac{1}{6}\frac{a^6 B_o^2 \sin^2\chi}{Ic^3}\omega^3 \qquad (4\text{-}12)$$

or, since $P = 2\pi\omega^{-1}$ and $\dot{P} = -2\pi\omega^{-2}\dot{\omega}$,

$$\dot{P} = \frac{1}{24\pi^2}\frac{a^6 B_o^2 \sin^2\chi}{Ic^3} P^{-1} \qquad (4\text{-}13)$$

That all period derivatives are positive is heartening at this point (it seems to at least confirm that a spinning body is involved); however the fact that there is no marked correlation of P and $\dot{P}$ implies that if the basic power-loss mechanism is magnetic-dipole radiation, the parameters a, B_o, $\sin\chi$, and I vary widely from pulsar to pulsar. For a "canonical" pulsar with $\sin\chi = 1$, $a = 10^6$ cm, and $I = 10^{45}$ gcm^2, we have (Manchester and Taylor 1977, p. 177), for P in seconds,

$$B_o \simeq 3.2 \times 10^{19}(P\dot{P})^{\frac{1}{2}} \text{ G} \qquad (4\text{-}14)$$

which gives values between about 2×10^{10} G and 2×10^{13} G, with 10^{12} G being typical. Using these "typical" values in (4-11), one finds that by this mechanism the Crab pulsar would put out about 7×10^{38} erg-s^{-1}, which is just about what is needed.

A further insight into pulsar emission processes can be gained by hypothesizing that for a pulsar with given parameters (which fix the constant K), the torque slowing rotation will be proportional to a power of the rotation frequency, so that

$$\dot{\omega} = -K\omega^n \qquad (4\text{-}15)$$

n being called the braking index. For magnetic dipole radiation we have seen that n = 3. Differentiation of (4-15) and elimination of K

give

$$n = \frac{\omega\ddot{\omega}}{\dot{\omega}^2} \tag{4-16}$$

so that the braking index can be determined from timing results if they are good enough to give a second period (or frequency) derivative. For example the braking index of the Crab Pulsar P0531+21, calculated from recent timing results (Groth 1975), is 2.5071. This has been seen as indicating that the magnetic dipole model serves as a good starting place in constructing pulsar models. It is rather disturbing that second derivatives recently published for 9 other pulsars (Gullahorn and Rankin 1978b) lead to very large braking indices (Appendix 2).

If the constant K in equation (4-15) is indeed constant throughout the life of a pulsar, (4-15) may be integrated to give an expression for the pulsar age t:

$$t = -\frac{\omega}{(n-1)\dot{\omega}}\left[1 - \left(\frac{\omega}{\omega_o}\right)^{n-1}\right] \tag{4-17}$$

where ω_o is the "birth" rotation frequency. If $\omega << \omega_o$ this age is approximately equal to the characteristic age for index n:

$$\tau \quad -\frac{\omega}{(n-1)\dot{\omega}} = \frac{P}{(n-1)\dot{P}} \tag{4-18}$$

Our previous definition of characteristic age as $\frac{1}{2} P\dot{P}^{-1}$ is simply τ for n = 3.

A simple argument (Canuto 1975c) about the magnitude of the "birth" rotation frequency is that it is, at maximum, that frequency corresponding to breakup (against Newtonian gravity) by centripetal forces, so

$$\frac{GM}{a^2} = \frac{v^2}{a} = \omega_o{}^2 a,$$

or $$\omega_o{}^2 = G\rho \qquad (4\text{-}19)$$

where $\rho \simeq Ma^{-3}$. At a density of 10^{15} g cm^{-3} and for a $\simeq$10 km, ω_o would be 10^4 rad s^{-1}, so that even for the Crab ($\omega \simeq 33 \times 2\pi$ rad s^{-1}), $\omega << \omega_o$. Canuto points out that expansion velocities observed in the Crab and Vela supernova remnants would also be consistent with an ω_o of this size.

The above considerations are for a rotator in vacuo, but the creation, due to the parallel component of the electric field, of a plasma atmosphere about the neutron star, will change the equations to be satisfied in the vicinity of the star. In particular source densities in Maxwell's equations will be non-zero. The solution to the entire problem will then differ from what has been described. The magnitude of the source densities will determine how much the models differ from the vacuum oblique rotator.

Magnetospheric Equations

To consider the effects of source densities, the following discussion, based on Cowling (1976) and Israel (1974) is offered.

The field equations with sources are

$$\nabla \times \bar{B} = \frac{4\pi}{c} \bar{j} + \frac{1}{c} \frac{\partial \bar{E}}{\partial t} \qquad (4\text{-}20)$$

$$\nabla \times \bar{E} = - \frac{1}{c} \frac{\partial \bar{B}}{\partial t} \qquad (4\text{-}21)$$

$$\nabla \cdot \bar{B} = 0, \quad \nabla \cdot E = 4\pi\rho \qquad (4\text{-}22)$$

and the generalized Ohm's Law is

$$\bar{j} = \sigma(\bar{E} + \frac{\bar{v}}{c} \times \bar{B}) \tag{4-23}$$

Equating the currents in (4-20) and (4-23), taking the curl, and using (4-21) and (4-22) to simplify the resulting $\nabla \times (\nabla \times \bar{B})$ and $\nabla \times \bar{E}$ terms, one obtains

$$\frac{\partial \bar{B}}{\partial t} = \nabla \times (\bar{v} \times \bar{B}) + \eta(\nabla^2 - \frac{1}{c^2} \frac{\partial^2}{\partial t^2}) \bar{B} \tag{4-24}$$

where $\eta = \frac{c^2}{4\pi\sigma}$ is the magnetic diffusivity. Ignoring the second-order time derivative of $\bar{B}$, which is due to displacement currents, should be valid where $\beta^2 << 1$ (Jackson 1975, p. 471). In any case, the plasma around a neutron star would be expected to have a very high conductivity, so that $\eta << 1$ and the second term may be neglected. The resulting

$$\frac{\partial \bar{B}}{\partial t} = \nabla \times (\bar{v} \times \bar{B}) \tag{4-25}$$

may be shown, by considering the flux traversing any moving surface in the plasma (Alfven and Falthammar 1963, p. 101), to imply that the magnetic field is "frozen into" the plasma. By using (4-21), the fact that this implies that the Lorentz force is zero (the "hydromagnetic condition"), may be easily noted. Obviously a way of checking models based on a vanishing Lorentz force ("force-free magnetospheres") would be to check that the conditions in the model, once solved, are such that the second term in (4-24) is negligible.

The case of near perfect conductivity and a magnetosphere corotating with the neutron star due to the freezing in of the magnetic field will now be considered.

The structure of the magnetosphere near the neutron star will now be considered, based on equations given in Scharlemann and Wagoner (1973) and Brooks (1974). A steady-state solution for a time-independent aligned rotator will be sought, with the assumptions that only electrons and a single ion species are present with well-defined bulk velocities, and that gravitational and inertial forces may be neglected. Complications which make the structure of the outer magnetosphere non-trivial are mentioned, but only the near magnetosphere is considered in detail.

In the inertial frame, the Lorentz force has form:

$$-en_-[\bar{E} + (\bar{\beta}_- \times \bar{B}) = m_-c^2 n_- \bar{\beta}_- \cdot \nabla(\gamma\bar{\beta})_- \qquad (4\text{-}26)$$

$$Zen_+[\bar{E} + (\bar{\beta}_+ \times \bar{B}) = m_+c^2 n_+ \bar{\beta}_+ \cdot \nabla(\gamma\bar{\beta})_+ \qquad (4\text{-}27)$$

so these are the equations of motion of electrons and ions of number densities n_- and n_+, masses m_- and m_+, and velocities, $v_\pm = \beta_\pm c$ respectively. The derivative $\frac{\partial}{\partial t}$ is zero, so the RHS is the "inertial force term" of the convective derivative $m\frac{d\bar{v}}{dt} = m(\frac{\partial \bar{v}}{\partial t} + \bar{v}\cdot\nabla\bar{v})$.

Neglecting the inertial force term is equivalent to assuming massless particles. This may be realistic where $\frac{B^2}{4\pi} << \gamma\mu c^2$ (μ = mass density), and in turn implies infinite conductivity (collisions are neglected), so that either algebraically, or arguing that the Lorentz force must vanish for the case of infinite conductivity, we obtain the condition mentioned after (4-25),

$$\bar{E} = -\bar{\beta}_\pm \times \bar{B} \qquad (4\text{-}28)$$

Neglect of inertial force terms also brings in an indeterminacy of electron and ion velocities - only the current $\bar{j} = e(Zn_+\beta_+ - n_-\beta_-)$, which is a linear combination of the desired velocities, is specified (Scharlemann 1974).

Maxwell's equations

$$\nabla\cdot\bar{B} = 0 \longrightarrow \bar{B} = \nabla \times \bar{A} \tag{4-29}$$

$$\nabla\cdot\bar{E} = 4\pi\rho = 4\pi e[Zn_+ - n_-] \tag{4-30}$$

are independent of assumptions, while

$$\nabla \times \bar{B} = \frac{1}{c}\frac{\partial\bar{E}}{\partial t} + \frac{4\pi}{c} j \tag{4-31}$$

in this case becomes

$$\nabla \times \bar{B} = 4\pi e(Zn_+\bar{\beta}_+ - n_-\bar{\beta}_-). \tag{4-32}$$

The remaining Maxwell equation:

$$\nabla \times \bar{E} = -\frac{\partial\bar{B}}{\partial t} \tag{4-33}$$

implies that $\nabla \times \bar{E} = 0$, so that $\bar{E} = -\nabla\Phi$.

Equation (4-28), as we have seen, implies that $\bar{E}\cdot\bar{B} = 0$: the magnetic field lines are equipotentials if (4-28) holds. It has already been shown to imply that the magnetic field lines are frozen into the plasma.

Equation (4-32), crossed into $\bar{B}$ gives

$$(\nabla \times \bar{B}) \times \bar{B} = 4\pi e(Zn_+\bar{\beta}_+ - n_-\bar{\beta}_-) \times \bar{B} \tag{4-34}$$

which using (4-26) and (4-27) becomes

$$(\nabla \times \bar{B}) \times \bar{B} = -4\pi e(Zn_+ - n_-)\bar{E} = -(\nabla \cdot \bar{E})\bar{E} \qquad (4\text{-}35)$$

so

$$(\nabla \cdot \bar{E})\bar{E} + (\nabla \times \bar{B}) \times \bar{B} = 0 \qquad (4\text{-}36)$$

or if $\frac{\partial}{\partial t} \neq 0$

$$(\nabla \cdot \bar{E})\bar{E} + (\nabla \times \bar{B} - \frac{1}{c}\frac{\partial \bar{E}}{\partial t}) \times \bar{B} = 0 \qquad (4\text{-}36a)$$

(Mestel 1973). This is the equation of a force-free electromagnetic field.

The axially symmetric corotating magnetosphere (Goldreich and Julian 1969) has no toroidal electric field component for the same reason that the aligned vacuum dipole did not, assuming $\frac{\partial}{\partial \phi} = \frac{\partial}{\partial t} = 0$. (A looser condition, $\frac{\partial}{\partial t} = -\omega\frac{\partial}{\partial \phi}$, is considered by Mestel (1971, 1973).) $\bar{E}_\phi = -(\bar{\beta} \times \bar{B})_\phi$ from (4-28), and if $\frac{\partial}{\partial t} = 0$, (4-25) shows that $\bar{\beta} \times \bar{B}$ is curl-free (solenoidal). Writing the vectors as the sum of poloidal $(\bar{\beta}_p, \bar{B}_p)$ and toroidal $(\beta_\phi\hat{\phi}, B_\phi\hat{\phi})$ vectors, one obtains (Mestel 1961)

$$\nabla \times (\bar{\beta}_p \times \bar{B}_p) = 0 \qquad (4\text{-}37)$$

and

$$\nabla \times (\beta_\phi\hat{\phi} \times \bar{B}_p + \bar{\beta}_p \times B_\phi\hat{\phi}) = 0. \qquad (4\text{-}38)$$

$\bar{\beta}_p \times \bar{B}_p$ is a toroidal vector (it is actually E_ϕ), and being solenoidal, must be the ϕ-derivative of a scalar function, which by axial symmetry is zero. Thus $\bar{\beta}_p \times \bar{B}_p = 0$, or $\bar{\beta}_p = K\bar{B}_p$ where K is a scalar. Since $\bar{B}_p = \bar{B} - B_\phi\hat{\phi}$, $\bar{\beta}$ may be written $\bar{\beta} = K(\bar{B} - B_\phi\hat{\phi}) + \alpha\hat{\phi}$, which may be put into (4-28) to yield

$$\bar{E} = (KB_\phi\hat{\phi} - \alpha\hat{\phi}) \times \bar{B}_p. \qquad (4\text{-}39)$$

To determine the scalar α we note that $\beta = \beta_\phi \hat{\phi} + \bar{\beta}_p$ where $\beta_\phi = \frac{\omega r \sin\theta}{c}$ for corotation at radius r. Then $\alpha = K\beta_\phi + \frac{\omega r \sin\theta}{c}$, so that

$$\bar{\beta} = K\bar{B} + \frac{\omega r \sin\theta}{c}\hat{\phi} = K\bar{B} + \frac{\bar{\omega} \times \bar{r}}{c} . \qquad (4\text{-}40)$$

We are now in a position to find $\bar{E}$ and the charge density which it implies. Since $\bar{E} = -\bar{\beta} \times \bar{B}$, the divergence of $\bar{E}$ is

$$\nabla\cdot\bar{E} = -\nabla\cdot(\frac{\bar{\omega} \times \bar{r}}{c} \times \bar{B}) = -\bar{B}\cdot\nabla \times (\frac{\bar{\omega} \times \bar{r}}{c}) + \frac{\omega r \sin\theta}{c}\hat{\phi}\cdot(\nabla \times B) \qquad (4\text{-}41)$$

In a non-charge-separated atmosphere where $\beta_+ = \beta_-$ in bulk, or in a highly charge-separated region where either n_+ or n_- may be neglected, (4-32) and (4-30) imply that

$$\nabla \times \bar{B} = \bar{\beta}\nabla\cdot\bar{E} \qquad (4\text{-}42)$$

and expanding $\nabla \times (\bar{\omega} \times \bar{r})$, noting $\bar{\omega} = \omega\hat{z}$,

$$(\nabla\cdot\bar{E})[1 - \frac{\omega r \sin\theta}{c}\hat{\phi}\cdot\bar{\beta}] = -\frac{\bar{B}}{c}[\bar{\omega}(\nabla\cdot\bar{r}) - (\bar{\omega}\cdot\bar{r})\bar{r}] = -2\bar{B}\cdot\bar{\omega}/c \qquad (4\text{-}43)$$

so that

$$\rho = \frac{\nabla\cdot\bar{E}}{4\pi} = -\frac{\bar{B}\cdot\bar{\omega}}{2\pi c}[1 - \frac{\omega^2 r^2 \sin^2\theta}{c^2}]^{-1} \qquad (4\text{-}44)$$

This is the charge density derived by Goldreich and Julian for a perfectly conducting corotating magnetosphere. Corotation cannot hold out to the light cylinder (the locus where $\omega r \sin\theta = c$), and indeed the toroidal current associated with the space charge in (4-43) becomes a major source of field near the light cylinder, distorting the dipole field.

Neglecting this distortion one can delineate the zone of corotation roughly by that dipole field line which first touches the light cylinder. A line touching the stellar surface at colatitude θ_o has a parametric equation (Lorrain and Corson 1970, p. 69; Jackson 1976)

$$r = a\left(\frac{\sin\theta}{\sin\theta_o}\right)^2. \tag{4-45}$$

Setting $r = c/\omega$ at $\sin\theta = 1$ gives the value $\sin\theta_o = \left(\frac{a\omega}{c}\right)^{\frac{1}{2}}$ and allows the polar equation of the edge of the CRM to be given;

$$r_{CRM} = \frac{c\sin^2\theta}{\omega} \tag{4-46}$$

The surface region where $\theta < \theta_o$ defines a "polar cap" of the pulsar, of radius (Ruderman and Sutherland 1975)

$$r_p = a\left(\frac{\omega a}{c}\right)^{\frac{1}{2}} \simeq 1.4 \times 10^4 \, P^{-1} \text{ cm}. \tag{4-47}$$

Mestel (1971) has pointed out the conditions to be found in such a corotating magnetosphere. The charge density is the excess of positive over negative charges, but the actual situation is believed to be one of large charge separation. This is equivalent to the assumption that electric fields due to space charge densities are negligible in comparison to the field implied by the force-free condition. In this case the ratio of the (excess) charge density to that of positive charge, $|\rho|/n_+Ze$, will be at least of order unity. In contrast, this ratio in a normal plasma would be far less than unity.

Using (4-44) in the form $|\rho| \simeq \frac{B\omega}{2\pi c}$, and noting that the ionic number density $n_+ = \frac{\rho_m}{Am_H}$, where A is the mass number of the ions, m_H the mass of a hydrogen atom, and ρ_m the mass density,

$$\frac{|\rho|}{n_+ Ze} \simeq \frac{B\omega}{2\pi c}\left[\frac{\rho_m Ze}{Am_H}\right]^{-1} = \left(\frac{B^2}{2\pi\rho_m c^2}\right)\left(\frac{\omega}{ZeB/Am_H c}\right) = 4\,\frac{B^2}{8\pi\rho_m c^2}\,\frac{\omega}{\omega_i} \tag{4-48}$$

where $\omega_i = \frac{ZeB}{Am_H c}$ is the gyration frequency of the ions. Since $\frac{\omega}{\omega_i}$ will be of order 10^{-16}, one is assured that the macroscopic equations (4-30) and (4-32) are valid. We have already concluded that the density of the plasma is such that the left-hand side of (4-48) is of order unity. Then the ratio of magnetic to rest mass energy,

$$\frac{B^2}{8\pi\rho c^2} \simeq 0\left(\frac{\omega_i}{\omega}\right) >> 1. \tag{4-49}$$

As seen in Chapter 3 this implies that the particle motions are relativistic. Mestel also shows that the convection current $\rho\bar{v}$ is effectively the total current, and that the electrical force density $\rho\bar{E}$ is nearly equal and opposite to the magnetic one, $\bar{j} \times \bar{B}/c$ (as expected from the force-free condition). From this the field is deduced to be nearly curl-free within the light cylinder:

$$r\sin\theta\,\frac{|\nabla \times B|}{B} \simeq 0\left(\frac{v}{c}\right)^2. \tag{4-50}$$

As mentioned, near the light cylinder corotation currents become important and distort an assumed dipole field.

Beyond the light cylinder the force-free condition may still be assumed - the restriction that $\beta < 1$ will then allow the shape of the field to be roughly determined. Equation (4-43) will still be useful in determining the charge density, but in (4-40) the value of K cannot be zero; (4-40) may be rewritten as

$$\bar{\beta}_p = K\bar{B}_p$$

$$\beta_\phi = KB_\phi + \frac{\omega r \sin\theta}{c}. \tag{4-51}$$

Since K is scalar (cf. eq. 4-39) $\bar{\beta}_p = K\bar{B}_p$, and

$$\frac{B_\phi}{B_p} = \frac{\beta_\phi - \frac{\omega r \sin\theta}{c}}{\beta_p} \tag{4-52}$$

Assuming $0 < \beta_\phi < 1$, some manipulation of inequalities yields

$$\left(\frac{B_\phi}{B_p}\right)^2 \geq \left(\frac{\omega r \sin\theta}{c}\right)^2 - 1$$

so that

$$-\frac{B_\phi}{B_p} \leq \left[\left(\frac{\omega r \sin\theta}{c}\right)^2 - 1\right]^{\frac{1}{2}} \tag{4-53}$$

is a strict inequality, for $\frac{\omega r \sin\theta}{c} > 1$.

If the field lines remain equipotentials, as assumed, they cannot close beyond the light cylinder, as charges could then corotate at superluminal speed. Rather, they must be swept back, so that $|B_\phi/B_p|$ grows large. Charged particles moving on such open lines could escape to the interstellar medium.

The basic structure which has been deduced for the magnetic field of an aligned rotator is illustrated in Figure 9. The basic structure of the corotating magnetosphere, under the assumptions of negligible space charges and currents and a force-free condition, have been adopted basically unchanged in many recent models (see Manchester and Taylor, pp. 181-182). However, the structure of the polar region and of the wind zone (the region outside the CRM), and the fitting

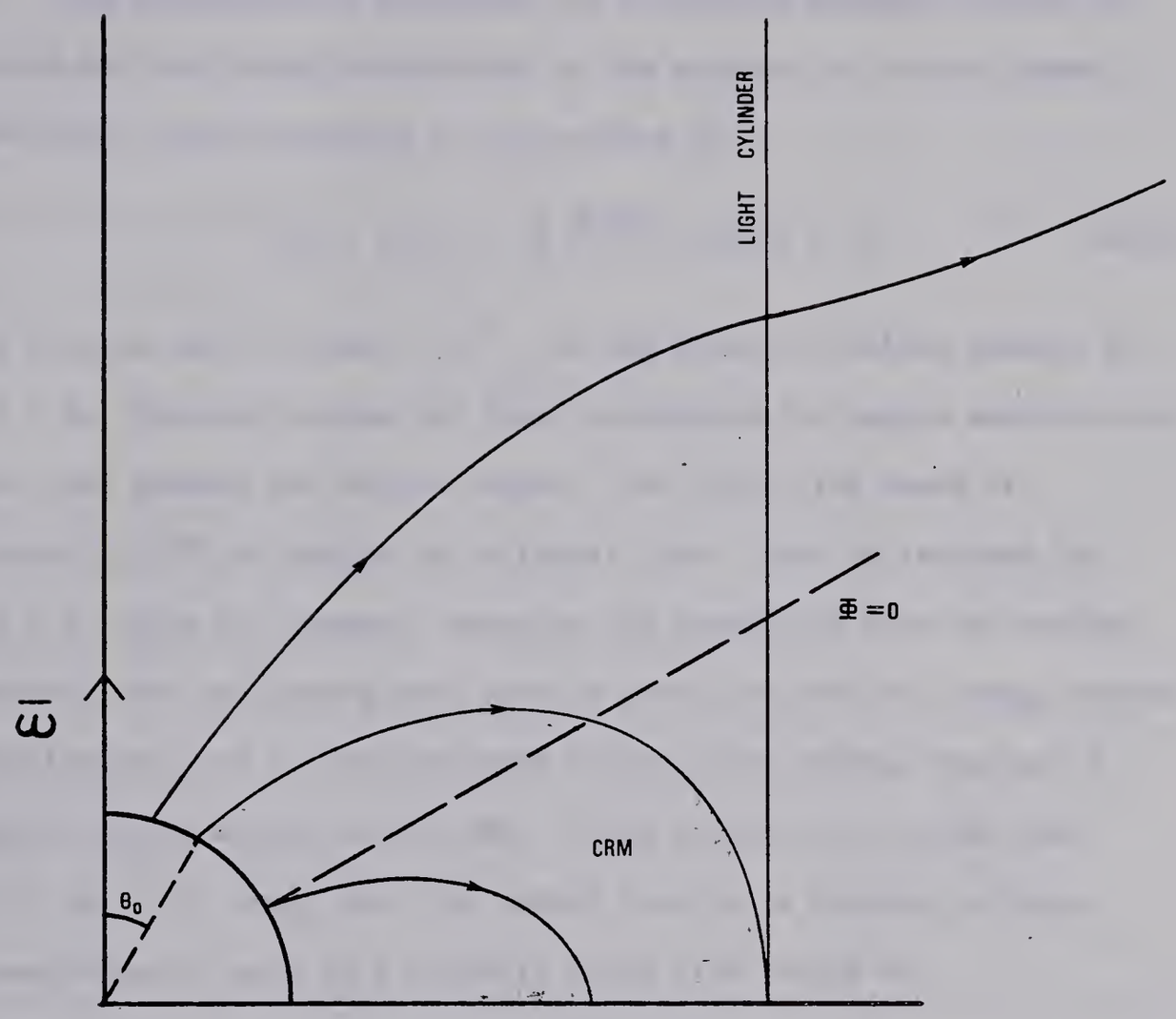

Figure 9. Magnetic field structure near a pulsar (aligned). Poloidal B only shown.

together of these structures with the CRM, vary from model to model.

The electrostatic potential for a rotating magnetic dipole in vacuum may not change drastically in the presence of a thin plasma. From (4-5), this potential at the surface is

$$\Phi(r = a,\theta) = -\frac{1}{6}\frac{B_o\omega a^2}{c}(3\cos^2\theta - 1), \qquad (4\text{-}54)$$

and thus is zero for $\cos\theta = 3^{-\frac{1}{2}}$. In the Goldreich-Julian theory, for $\bar{\omega}\cdot\bar{\mu} > 0$, electrons stream out from the surface for angles smaller than this, and protons for angles larger. The field line based at $\theta = \cos^{-1}(3^{-\frac{1}{2}})$ is called the critical line. This is reversed for $\bar{\omega}\cdot\bar{\mu} < 0$. This is, however, based on the assumption that the surface potential for the vacuum case carries over, and with the charge density (4-44) implies that in certain cases charges flow through regions of opposite space charge in the CRM. There is also the problem that (4-9) and (4-4) imply that the radial force on a charged particle (constrained to move on a magnetic field line) would be

$$F_r\alpha - \cos^4\theta q$$

so that only charges of $q < 0$ (electrons) would be accelerated away from the surface. The fact that for $\cos\theta > 3^{-\frac{1}{2}}$ positive charges at the pulsar surface have larger energy than they would if allowed to escape to infinity does not matter, the local field will not allow them to stream out as envisaged by Goldreich and Julian. Again if $\bar{\omega}\cdot\bar{\mu} < 0$ the opposite is true - electrons would be held in by the field. The role of stellar charge in removing this problem will be discussed in later pages.

The difference in ionic and electronic work functions, discussed in Chapter 3, has entered some recent models (Ruderman and Sutherland 1975; Jackson 1976) in an important role. These models will be discussed in the following pages. The ratio of ion to electron field emission currents in applied electric fields of the same magnitude will very roughly be

$$\exp\left[-\left(\frac{m_i}{m_e}\right)^{\frac{1}{2}} \left(\frac{\phi_i}{\phi_e}\right)^{\frac{3}{2}} \frac{1}{Z_c}\right]$$

where m_i/m_e and ϕ_i/ϕ_e are the mass and work function ratios, and both ion and electron emission are assumed to follow the Fowler-Nordheim equation (Gomer 1961, p. 9). The ion charge is Z_c.

Field emission of electrons, given the mass and work function differences from ions, should be very easy compared to that of ions. This is largely due to the tunneling ability of the less massive electrons. The treatment of pulsar surfaces as electron-emissive but ion-retentive is justified at the temperatures which characterize most of the surface.

Rarified Magnetosphere

Jackson (1976) considers a slowly rotating aligned magnetic dipole surrounded by a tenuous atmosphere in which the force-free condition does not hold. As an initial approximation the vacuum electric potential is, for $\bar{\omega}\cdot\bar{\mu} > 0$,

$$\Phi(r > a,\theta) = \frac{\omega B_o a^3}{cr}\left[\varepsilon - \frac{1}{3}\left(\frac{a}{r}\right)^2 P_2(\cos\theta)\right], \qquad (4\text{-}55)$$

where the star has a charge $\varepsilon\frac{\omega B_o a^3}{c}$, with ε to be determined. The

magnetic dipole has an electric monopole superposed on it. The radial dependence is such that the electric monopole dominates the motion of charged particles at large radii.

In a similar manner to that of the Goldreich-Julian model, electrons are emitted from the polar region if $0 < \varepsilon < 1$. The magnitude of electron emission current densities will be much greater than that for ions due to the difference in work functions. At the surface

$$\bar{E}\cdot\bar{B} \propto [\varepsilon - (\frac{a}{r})^2 \cos^2\theta](\frac{a}{r})^5 \cos\theta \qquad (4\text{-}56)$$

so that positive charges are emitted for $\theta > \cos^{-1}(\varepsilon^{\frac{1}{2}})$. These are bound to move on the magnetic surfaces of (4-45), and remain within

$$r_{max} = a \frac{1}{\sin^2(\cos^{-2}(\frac{1}{2}))} = \frac{a}{1 - \varepsilon} \qquad (4\text{-}57)$$

of the star. The electrons, emitted near the pole, can move to very large radii where they feel only the asymptotic Coulomb field of the star until they merge into the perfectly conducting interstellar medium at radius R_N. In the steady state the potentials of the polar cap and that of the interstellar medium have been equilibrated by the electron current so that the charge of the star undergoes no further changes. This allows ε to be determined with (4-55) as

$$\varepsilon \simeq \frac{R_N}{a}[\varepsilon - \tfrac{1}{3}]$$

or

$$\varepsilon \simeq \tfrac{1}{3}(1 - \frac{a}{R_N})^{-1} \sim \tfrac{1}{3}. \qquad (4\text{-}58)$$

To stress the zones of dominance of the magnetic dipole and electric monopole terms, respectively, Jackson defines a magnetic flow region (MFR), where $|\bar{E} \times \bar{B}| > E^2$ and an electric flow region (EFR), where $|\bar{E} \times \bar{B}| < \bar{E}^2$ (see also Jackson 1975, p. 583). The boundaries of these, and the surface $|\bar{E}| = |\bar{B}|$, are approximately:

$$\text{MFR:} \quad \sin\theta > \frac{2Er}{\rho_\ell} \left[1 - \varepsilon^{-1}\left(\frac{a}{r}\right)^2 2P_2(\cos\theta)\right]$$

$$\text{EFR:} \quad r > \frac{3}{2}\rho_\ell \frac{(1 + 3\cos^2\theta)}{\sin\theta} \qquad (4\text{-}59)$$

$$\text{E=B:} \quad r = \frac{3}{2}\rho_\ell (1 + 3\cos^2\theta)^{\frac{1}{2}}$$

where $\rho_\ell = \frac{c}{\omega}$ is the light cylinder radius.

Although once ε has taken its equilibrium value the electrons will no longer reach the interstellar medium, they are still emitted at the pole. Their subsequent motion causes current loops from above the pole back to the star. Using (4-55) it is readily shown for $\varepsilon = \frac{1}{3}$ that, in travelling along a magnetic field line near the star, a particle finds itself at the same electrical potential as at the surface (i.e., $\Delta\Phi = 0$ when it has reached $\theta = \sin^{-1}(\frac{2}{3})$. If, however, it enters the EFR before reaching this "standstill" point, it will feel an electric force which will dominate its motion and cause it to move to magnetic surfaces with a larger θ_o. Jackson then envisages motion along these surfaces back to the star to form a current loop.

As a higher-order effect of rotation, Jackson considers the atmospheric charge distribution. As (4-56) shows $\bar{E}\cdot\bar{B} = 0$ on the loci $\theta = \frac{\pi}{2}$ (the equatorial plane) and

$$r_o = a\varepsilon^{-\frac{1}{2}}\cos\theta, \qquad (4\text{-}60)$$

a circle of radius $\frac{a}{2}\epsilon^{-\frac{1}{2}}$ centred at $Z = \frac{a}{2}\epsilon^{-\frac{1}{2}}$. Charges near one of these loci would feel a force towards these $\bar{E}\cdot\bar{B} = 0$ surfaces. If any energy dissipation mechanism is available the particles will settle onto the $\bar{E}\cdot\bar{B} = 0$ surface as a minimum of their electrostatic energy. Jackson suggests curvature radiation (to be discussed) as a dissipation mechanism to allow the formation of an electron cloud about a polar dome, and an ion cloud in the equatorial plane, and points out that the exact dynamics of the particles would be an extremely complicated problem. This picture of a low density magnetosphere is given in Figure 10. The negative charges along $\bar{E}\cdot\bar{B} = 0$ form a dome, above and below which the charge density should be very small. Since Jackson considers densities which are undoubtedly orders of magnitude lower than those of the Goldreich-Julian model, vacuum dipole radiation would be the main energy loss mechanism in this model (see Ostriker and Gunn 1969; Gunn and Ostriker 1970). It is a self-consistent model and is physically reasonable - Jackson suggests that the basic morphology will remain even in higher density regimes. That this is true when rotation is rapid and the light cylinder near the star is very doubtful. Nevertheless the suggestion that the stellar charge must be non-zero, which also characterizes oblique rotators (Jackson 1978b), and that the monopole field due to this charge should dominate motion of charged particles at large radii, is likely valid. In addition, (4-56) clearly defines zones of electron and ion emission due to surface fields, which it was noted is a feature lacking in the Goldreich-Julian model.

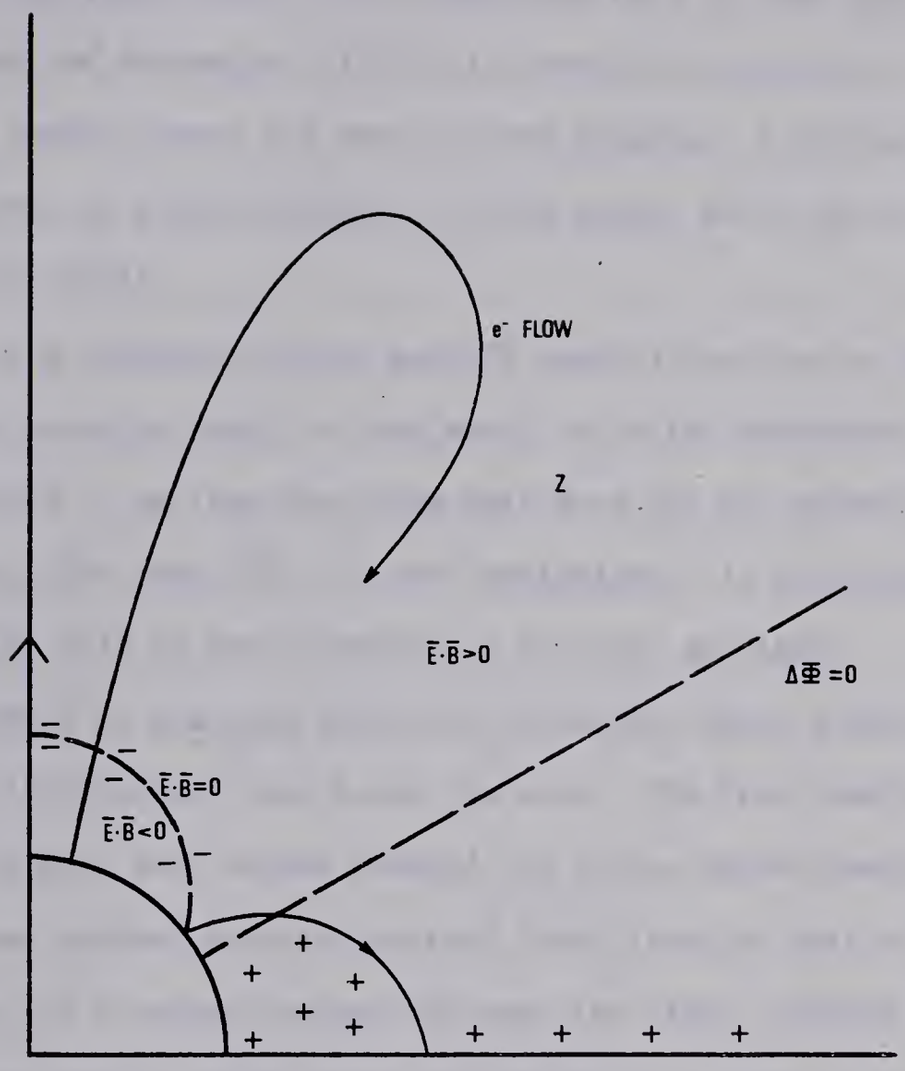

Figure 10. Jackson magnetosphere.

The Ruderman-Sutherland Model

The final model to be considered here in some detail is that of Ruderman and Sutherland (1975), in which the retention of ions at a pulsar surface shows its most extreme effects. Pair production above polar caps is a major feature of this model, as it is of the model of Sturrock (1971).

The Goldreich-Julian model's general features as described earlier are also basic to this model, with the important restriction that $\bar{\omega}\cdot\bar{\mu} < 0$, so that the poles emit ions (to the extent that this occurs). The case $\bar{\omega}\cdot\bar{\mu} > 0$, the "antipulsar," is not considered here, since the role of ion retention is then not so clear.

Most of the open lines are lines onto which a small ion current may be injected and thus leave the star. The first implication is that the star will become charged, as in the Jackson model. It is then not clear whether positive current loops from the pole to a polar annulus, or a current stream out past the light cylinder would form. In either case a region where due either to a strong parallel component of the electric field (Jackson), or the need to resupply to the magnetosphere charges lost through the light cylinder (Goldreich and Julian), a strong positive currently radially outward from the polar cap exists, if the surface supplies ions. Neglecting the effects of its own magnetic field, the current flowing from the polar cap can have a maximum rate, in particles per second, of

$$\dot{N}_{max} \simeq \pi r_p^2 \frac{\bar{\omega}\cdot\bar{B}_o}{2\pi ec} c. \qquad (4\text{-}61)$$

This would correspond to the local charge density of (4-44) moving outward above the polar cap at speed c. In a steady-state situation where the surface could supply ions at any rate, even particle fluxes as high as that in (4-61) could flow away from the pole without the local density being changed. However, if ions are not readily available, the region above the polar cap will be depleted of particles completely. This is due to the electric field acting on the charge-separated plasma above the polar cap, and what happens to particles cleared out of the gap does not matter at this stage of the discussion.

Ruderman and Sutherland (1975) have solved the problem of a magnetosphere separated from a neutron star by a spherical vacuum gap of height h, and find that the gap has a field and total potential drop, at the pole, of

$$E = \frac{2\omega \bar{B}_o}{c} h \qquad (4\text{-}62)$$

and

$$\Delta V = \frac{\omega \bar{B}_o}{c} h^2 \qquad (4\text{-}63)$$

respectively. In the more realistic case where a gap occurs only at the poles, (4-62) and (4-63) will be true near the centre of the gap, provided $h << r_p$. The top surface of the gap will consist of a plasma in which $\bar{E} \cdot \bar{B} = 0$. In addition, this condition that the magnetic field lines be equipotentials is met on the side of the gap, so that as the gap grows in height due to the loss of positive charges from the region of the pole, a cylindrical geometry, with this condition on the walls, becomes appropriate to the problem. Using this geometry, Ruderman and Sutherland find that a maximum potential difference of $\frac{\omega B_o}{2c} r_p^2$ can be

developed in a gap.

Michel (1979) discusses gap formation as a basic property of pulsar magnetospheres, capable of removing certain basic inconsistencies of force-free atmospheres. The Ruderman-Sutherland model is a special case in Michel's discussion although in his paper the existence of vacuum gaps is postulated without establishing a physical reason for their existence. In the preceding pages the ion retention of the pulsar surface has been shown to allow gap formation, so that Michel's study of the structure of such gaps is of interest in that it provides a complimentary approach to the problem.

The next consideration in the Ruderman-Sutherland model is the breakdown of the gap by pair production from γ-rays of energy greater than $2m_e c^2$ moving in the intense magnetic field. It is pointed out that even the natural background flux of such γ-rays exceeds 10^5 s^{-1} onto the polar cap. As pointed out by Sturrock (1971), Erber (1966) gave equations for pair production in intense magnetic fields. The created particles move in the gap electric field, acquiring an energy, from (4-63), of $\frac{\omega B_o h^2 e}{c}$ electron volts, which for the canonical pulsar parameters, and assuming $h \simeq 10^3$ cm, is 10^{11} eV (Ruderman and Sutherland 1975). These energetic particles in turn emit curvature radiation (see below) which allows the cycle to start again and continue to build up a large spark discharge.

To consider in further detail the mechanism of the spark, we now briefly discuss the processes involved. In the intense magnetic fields which are found near the neutron star, electrons and positrons will predominantly have the lowest of the discreet energies given by

(3-12) or (3-14). It is not immediately obvious why this is so, given that the particle energy could be of large magnitude even before acceleration by the field, and that a momentum component perpendicular to the field could be present and of large magnitude (Erber 1966). If the energy associated with this perpendicular (quantized) motion is of the same order as that with motion along the lines, one finds that if $\gamma^2 B >> 6 \times 10^{15}$ G, radiation formulae for strong coupling of particle and field must be used (Chiu 1972). The lifetime of an electron or positron in this regime has an upper limit of order $10^{-19} (B_q/B)^{2/3}$ s. Clearly a particle will leave this regime rather quickly, entering the quantum regime where lifetimes are of order $10^{-19} (B_q/B)^2$ s (Chiu 1972), so that the upper levels cannot remain populated. The observation in Her X-1 of a hard X-ray line by Trumper and his colleagues at the Max-Planck-Institut (1977), which they interpret as a Landau-level transition (see Chapters 1 and 3) could be due to this decay of the perpendicular energy of pair-produced particles. This hypothesis is advanced cautiously due to the fact that gas accretion in a binary X-ray pulsar such as Her X-1 (Manchester and Taylor 1977, pp. 85-87) could also supply particles capable of producing such a line. The detection of such lines in radio pulsars would support the hypothesis that pair production occurs, since it would provide a means of populating upper levels. What is clear, however, is that the bulk of the particles in motion along field lines will be in the lowest Landau level. Their radiation can no longer be considered classically, and the result of being in the lowest discreet level is that they do not radiate due to their motion around the field lines. However, in

following field lines, which are curved, they undergo an acceleration which is in the classical regime and may thus be treated by the theory of classical synchrotron radiation. The radius of curvature entering the synchrotron formulae will be ρ_f, the local radius of curvature of the field line which the particle is on. The characteristic energy radiated by a particle in such motion is (Jackson 1975, p. 675; Ruderman and Sutherland 1975):

$$E_{ph} = \hbar\omega \simeq \frac{3}{2}\gamma^3 \hbar c/\rho_f \tag{4-64}$$

and they are emitted within an angle γ^{-1} of the field line. Photons, either from external sources or from curvature radiation within a region of intense magnetic field, have mean free path due to pair production:

$$\text{for } \hbar\omega < 2mc^2 \qquad \ell = \infty$$

$$\hbar\omega > 2mc^2 \qquad \ell = \frac{4.4}{(e^2/hc)} \frac{\hbar}{mc} \frac{B_q}{B_\perp} \exp\left(\frac{4}{3\xi}\right) \tag{4-65}$$

(Ruderman and Sutherland 1975), where $\xi = \frac{\hbar\omega}{2mc^2} \frac{B_\perp}{B_q}$, and $B_\perp = B \sin\theta$, where θ is the angle between $\bar{B}$ and the photon propagation vector.

The particle multiplication factor needed for a discharge to occur is provided by the many photons of high energy emitted by a particle as curvature radiation. The energy loss rate (Jackson 1975, p. 661; Ruderman and Sutherland 1975),

$$P = \frac{2}{3} \frac{e^2}{c^3} \gamma^4 \left(\frac{c^2}{\rho_f}\right)^2 \tag{4-66}$$

if multiplied by hc^{-1}, the time spent traversing the gap, gives the

energy lost by one particle in the gap. Dividing by the mean photon energy from (4-64) the number of photons produced is approximated by

$$N_{ph} \simeq \frac{4}{g} \frac{e^2}{ch} \frac{h}{\rho_f} \gamma. \tag{4-67}$$

(Note error in eq. 25b, Ruderman and Sutherland 1975.) $N_{ph} >> 1$ is the condition for a discharge.

The gap height h is determined by requiring that $1 \simeq h$, and by using the mean photon energy (4-64) and an appropriate Lorentz factor corresponding to the traversal energy of the gap, producing a transcendental equation for h:

$$h^2 = 1.45 \exp ah^{-7} \tag{4-68}$$

where

$$\frac{1}{a} = \frac{9}{8} \left(\frac{e\omega B}{mc^3}\right)^3 \frac{\hbar c}{\rho_f} \frac{1}{2mc^2} \frac{1}{\rho_f} \frac{B}{B_q}. \tag{4-69}$$

The field line curvature radius ρ_f is assumed to be 10^6 cm in the polar gap, typical of higher-order multipole fields near the star. The value $\frac{h}{\rho_f}B$ is that of $B_\perp$ for a curvature radiation photon after going a distance h from its point of emission essentially tangent to a field line. Ruderman and Sutherland obtain values of $\xi^{-1} \simeq 15$ and

$$h \simeq 5 \times 10^3 \left(\frac{\rho_f}{10^6}\right)^{2/7} P^{3/7} B_{12}^{-4/7} \text{ cm} \tag{4-70}$$

for the gap. Using this value of h, the photon mean energy and the gap potential may be expressed in more fundamental units:

$$E_{ph} \simeq \omega^3 B^3 h^6 \rho_f^{-1} \propto (\rho_f^5 \omega^3 B^{-3})^{1/7} \tag{4-71}$$

and

$$\Delta V \simeq \frac{\omega B h^2}{c} = 1.6 \times 10^{12} B_{12}^{-1/7} \left(\frac{\rho_f}{10^6}\right)^{4/7} \text{ Volts.} \qquad (4\text{-}72)$$

For a canonical pulsar this potential difference would cause electrons or positrons to have Lorentz factors of order 10^6. A thin gap with this potential difference, and with $\bar{E}\cdot\bar{B} = 0$ in the plasma above it and at the top edge, will have a parallel electric field of magnitude

$$\bar{E}\cdot\hat{B} \simeq \frac{2\omega B}{c}(h - z), \qquad (4\text{-}73)$$

where z is the height in the gap from the surface. At the surface this field is about $\frac{\omega B h}{c}$, a factor $h/a \simeq 10^{-3}$ smaller than $\frac{\omega B a}{c}$ (i.e., about 10^9 Vcm^{-1}) which would typify a vacuum rotator. Thus with the binding energies for ions discussed in Chapter 3, ionic field emission from polar regions beneath such vacuum gaps would be totally negligible.

For the parameters just obtained, equation (4-67) gives a multiplication factor of 50 photons/particle, so that a discharge should easily be maintained.

The creation of pair-production discharges is illustrated in Figure 11, where a major problem may be seen. The discharge moves away from the centre of curvature of the field lines, and in the case of dipole field ends up on axis. Amplification along one field line does not occur, so that a shower, instead of a spark, occurs. Cheng and Ruderman (1977) suggest that the spark picture may be saved by the interaction of accelerated electrons with the surface, which will produce a γ-ray shower leading to further pair-creation near the field line on which the original pair was produced. It may also be that the

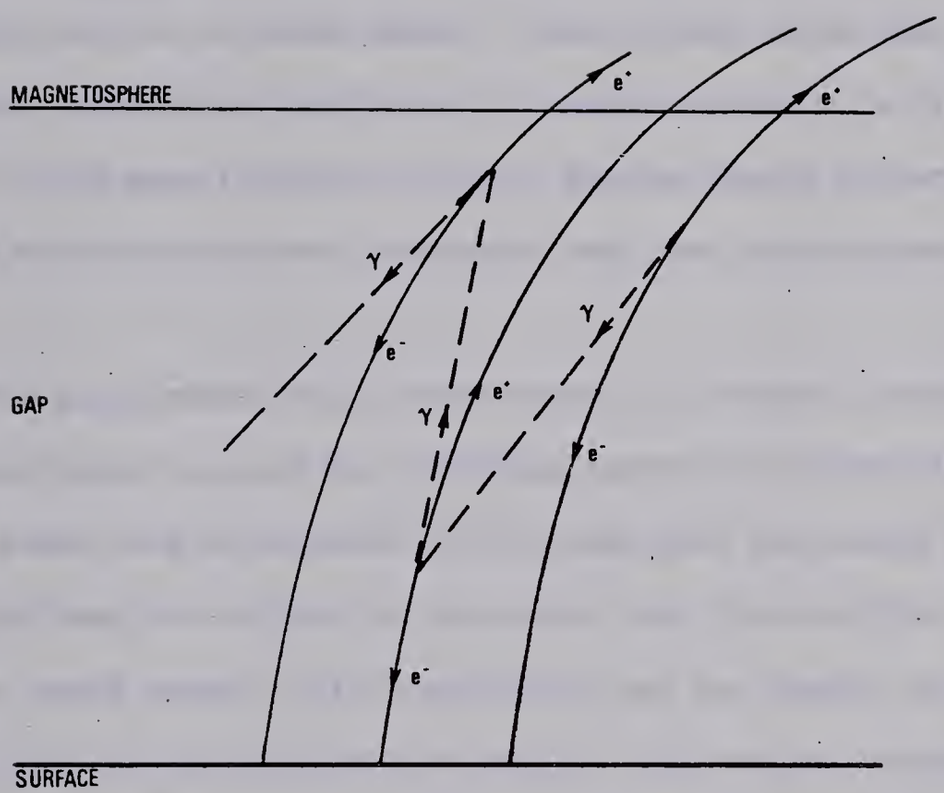

Figure 11. Pair-production discharges illustrating drift toward magnetic axis (after Cheng and Ruderman 1977b).

synchrotron radiation which may accompany the birth of a pair (as discussed earlier in this chapter) would be sufficiently energetic while the particle is in the strong-coupling regime that further pairs could be produced from it. It is worth noting that if $\gamma \simeq 10^5$ characterizes the energy of a newly formed pair, the energy $\hbar\omega_c = 116\ \gamma^2(\frac{B}{10^{13}})$ keV (Chiu 1971) which characterizes the critical frequency, will be of order $100mc^2$. Erber (1966) notes that the pair-production attenuation coefficient is maximized when $\hbar\omega = 12(\frac{B_q}{B})mc^2 \simeq 120mc^2$. The mean free path for such photons should be very short and thus allow further pair production very near the original field line.

The gap electric field accelerates the created electrons toward the polar cap, and the positrons toward the interstellar medium. Fawley, Arons, and Scharlemann (1977) claim that the inward electron flux would heat the surface to the extent that free ion flow (thermionic emission) would occur. This possibility, and the results of the positron flux to the interstellar medium, will now be considered.

Ruderman and Sutherland (1975) give as an estimate of the maximum ion flux at temperature T:

$$F(T) \simeq \frac{\rho_m}{m}(\frac{kT}{m})^{\frac{1}{2}} \exp(-\frac{E_B}{kT}) \qquad (4\text{-}74)$$

(see also Jenkins and Trodden 1965, p. 71), where m is the ion mass and ρ_m the mass density at the surface. E_B is the ionic binding energy, essentially the cohesive energy, and is in the range 2-10 keV. Due to the exponential term, only when $kT \simeq 8.6 \times 10^{-8}T$ keV also is of this order or greater, will there be essentially free thermionic ion

emission. The failure to observe X-ray emission has ruled out pulsar surface temperatures of this order. If the maximum polar current of equation (4-61) were due to thermionic ion emission, a temperature of order 6×10^6 K (Ruderman and Sutherland 1975) would be required at the cap. This appears to be observationally ruled out by an absence of X-ray emission. Of course, a consistent way of seeing what the temperatures are, is to calculate them based on the model being considered. Ruderman and Sutherland assume inflow of electrons at the local charge density of a force-free atmosphere, at speed c, to show what temperatures are to be expected. Assuming blackbody radiation as the only loss mechanism for the $\frac{1}{2}\Delta V \rho c$ erg $cm^{-2}s^{-1}$ flowing into the surface, a temperature of 2.4×10^6 K may be assigned to the cap. Although at this temperature thermionic ion emission could not supply ions at the rate of equation (4-61), it is clear that under these extreme circumstances ions could be emitted, thermionically, at the polar cap. The possibility that ion emission does occur, and its influence on pair-production discharges, is considered in Cheng and Ruderman (1977b). However, the assumption of Fawley et al. (1977) that ion emission at the polar caps is essentially free is not justified. This is seen even more clearly in noting that a pair-production discharge is needed in the first place to permit the heating of the cap to the point where any ions are emitted. There is major heating only in the fastest pulsars (Cheng and Ruderman 1977c) and the effects of the limited ion emission in others will not be discussed here.

An observable effect of positron outflow from the pulsar (or of Jackson's return currents) should be the presence of .511 MeV

annihilation radiation from pulsars. Such radiation is produced by either direct annihilation or the decay of singlet positronium which may be formed by the positrons with electrons from the interstellar medium. Triplet positronium, which decays into three γ-rays, giving a continuum spectrum, could be formed at the low densities in the interstellar medium (Ramaty and Lingenfelter 1979), but we shall assume that it is absent.

Again let us assume, as an extreme case, that the maximum charge loss of equation (4-61) occurs as positrons (there would also be a Goldreich-Julian type electron wind from lower-latitude field lines if a Jackson current loop is not present). Every positron will annihilate to produce two photons of .511 MeV, the distribution of which we may assume to be isotropic. Then at earth, a distance d from the annihilation region, the number flux of .511 MeV γ-rays will be

$$N \simeq r_p^2 \frac{\omega B_o}{e} (4\pi d^2)^{-1} \text{ cm}^{-2}\text{s}^{-1}, \tag{4-75}$$

or for a pulsar with r_p given by (4-47), $B_o \simeq 10^{12}$ G, and d in kpc:

$$N \simeq 2 \times 10^{-14} p^{-3} d^{-2} \text{ cm}^{-2}\text{s}^{-1}. \tag{4-76}$$

For the Crab (P0531+21) and Vela (P0833-45) pulsars this would imply that about 10^{-10} photons $\text{cm}^{-2}\text{s}^{-1}$ could be observed, while for the nearby pulsars (d = .1 kpc) P0950+08 and P1929+10, respectively 1.2×10^{-10} and 1.7×10^{-10} photons $\text{cm}^{-2}\text{s}^{-1}$ would be expected. The present limits to detection at .511 MeV are (liberally) 10^{-6} photons $\text{cm}^{-2}\text{s}^{-1}$ (HEAO-C should detect 10^{-4} to 10^{-5} $\text{cm}^{-2}\text{s}^{-1}$ over the range .06 to 10 MeV (Lingenfelter and Ramaty 1978)). The upcoming launches of

new satellites equipped to detect γ-ray lines should allow the detection of much lower levels of photon flux in the near future. The four pulsars mentioned will probably be the easiest to detect as they maximize $P^{-3}d^{-2}$.

Time Structure of Discharges

As the discharge proceeds, the gap potential is reduced steadily. The time scale for each stage of pair-production amplification is about $1/c \simeq h/c \simeq 10^{-6}$ s, the time it takes a curvature radiation photon to move through its mean free path. This is the time required for "tripling" - the particle which emitted the curvature radiation, plus a new pair, exist after this time. Once enough pairs have been produced that the force-free density is reached, the gap potential will be zero. Sometime shortly previous to this, pair production, and thus the growth of the discharge, stop. Ruderman and Sutherland (1975) estimate that 10^{15} pairs/cm^2 must be produced, which requires about 35 ($10^{15} \simeq e^{35} \simeq 3^{35}$) tripling times, or 10 μs. This is the time scale of the micropulses observed in many pulsars (see Chapter 1 and Manchester and Taylor, pp. 46-47). This time scale seems questionable: if each particle produces 50 photons, not a tripling but a hundredfold increase occurs at each step. 10 μs is an upper limit to the discharge time, if this simplistic discharge occurs (ignoring currents).

Once the discharge has taken place, the cycle starts over. As this restart is due to the magnetosphere demanding particles from the polar cap either for acceleration into interstellar space or for a

Jackson-type current, it is important to note that this demand for charges in a way not fully explained in this thesis is just as fundamental to pair-production through polar gap formation as is the basic reluctance of the surface to give up particles.

It is clear that the discharge time scale would be much less than that of the rotation of the neutron star, so that many discharges occur in one period. The pulses themselves are explained by a beam above the magnetic polar cap(s) swinging by us as the (oblique) rotator spins.

A further timing effect of this theory is that pulsars should turn off once their period becomes too long. It was seen (before equation 4-70) that $\xi^{-1} < 15$ is a condition for discharge. From this Ruderman and Sutherland find a critical period

$$P_{crit} = 1.7 B_{12}^{8/13} \left(\frac{a}{10^6}\right)^{21/13} \left(\frac{\rho_f}{10^6}\right)^{-4/13} (15\xi)^{-2/3} \text{ s} \qquad (4\text{-}77)$$

above which pair-production discharges do not occur. Using an equation similar to (4-14), and with a, ρ_f, and ξ assumed to be "typical," the result

$$P\dot{P} < \text{const } (P/\dot{P})^{-13/5}$$

is obtained. In 1975 this agreed well with the available data, and although modifications due to ion emission must be made (Cheng and Ruderman 1977b), it is a useful and testable aspect of this theory that it predicts effects which should be seen as correlations of timing results.

We now briefly consider the oblique rotator. Although Ruderman and Sutherland use an aligned rotator tilted slightly to represent an oblique rotator (and in so doing they derive expressions for the drift periods of drifting subpulses), this is clearly an oversimplification. For pair production to occur in aligned rotators we must have a region of ion retention above which positive charges are quickly swept away to form a gap. In the case where $\omega\mu < \bar{\omega}\cdot\bar{\mu} < 0$ and with no stellar charge, $\bar{E}\cdot\bar{B}$ would draw electrons from the star between the rotation and magnetic equators, and ions from the remainder of the stellar surface, but if the star has charge the situation becomes much more complex (Jackson 1978). Using the criterion of field lines closing at the light cylinder to define the polar cap borders, the radius of the polar cap would decrease as the obliquity increased, then increase again as $\chi \to \pi/2$. Jackson gives the value of the parallel component of $\bar{E}$ at the magnetic pole (again $\bar{\omega}\cdot\bar{\mu} < 0$) as

$$\bar{E}\cdot\hat{B} = -\frac{B_o \omega a}{c}\cos\theta. \qquad (4\text{-}79)$$

Since for $\theta_m = 0$, $\cos\theta = \cos\chi$ and is constant in time, the situation is similar to the aligned case, but the polar cap may not be spherical due to the lack of symmetry, and the field becomes small for large χ (as an extreme case consider $\chi = \frac{\pi}{2}$, where the radial electric field precisely at the magnetic pole is zero, and the ion-emissive part of the polar cap is a semi-circle. However as long as χ is not so large that the parallel electric field is too small, pair production discharges would still be expected in the oblique case.

To summarize, an aligned magnetic rotator with ion retention would be expected to form a force-free atmosphere near the star, and to have either charged particle loss along open field lines or looping currents in the outer magnetosphere, depending on the extent to which it is charged. In the special case that $\bar{\omega}\cdot\bar{\mu} < 0$ and that particle removal from the polar zone is very efficient, vacuum gaps will form above the magnetic poles, and discharge through pair production. The extension to oblique rotators is plausible. Observable signs that this mechanism is present would be lines from Landau level transitions of newly created particles, and .511 MeV radiation at a level below current detection limits. The radiation at other wavelengths which such a mechanism produces will be discussed in the next chapter.

CHAPTER 5

PULSE RADIATION MECHANISMS

This chapter will mainly extend the consideration of pair-production discharges to show that they could lead to pulsar radio emission.

That the radio emission from pulsars is coherent may be deduced from fluxes observed, combined with the fastest fluctuation time scales, of order 100 μs (Chapter 1). The size associated with such fluctuations is of order 10 km, and of course models which have been discussed are also of about this size. Knowing the distance from dispersion measures, a solid angle and thus intensity I_ν may be assigned to a pulsar. Radio brightness temperatures, $T_B = \frac{c^2 I_\nu}{\nu^2}$ which are calculated, are typically 10^{23} to 10^{28} K (Manchester and Taylor 1977, p. 201). An incoherent radiation mechanism could not account for brightness temperatures this high. Optical and X-ray emission, however, are probably incoherent, with brightness temperatures of only 10^{11} K.

The two possibilities for production of coherent radiation are stimulated emission and "antenna" mechanisms. Mechanisms involving stimulated emission are of two basic types, both of which may be classed as "maser amplification": direct amplification of electromagnetic waves, or plasma wave amplification followed by conversion to electromagnetic radiation (Manchester and Taylor 1977, p. 208). Chiu (1972; Chiu and Canuto 1971) has shown that the first mechanism may operate for steady electron streaming above polar caps, due to a population

inversion. Soviet workers have tended to favor the second mechanism and an origin of the pulsed radiation in the magnetosphere relatively far from the star (a "light cylinder" as opposed to "polar cap" origin) (Ginzberg and Zheleznyakov 1975). These maser mechanisms generally do not require special spatial distributions of radiating particles to function, and this may be seen as an asset. However, the physical conditions in the plasma for maser processes to occur are somewhat restrictive and not in all cases consistent with the generally assumed magnetospheric structure. Light cylinder models are particularly suspect due to possible breakdown of corotation (Mestel 1975; Jackson 1976). The aim of this discussion has been to mention that from maser processes there are useful emission theories which should be considered as strong competitors of the Ruderman-Sutherland theory, which itself is an antenna theory, involving the formation of particle bunches of diameters which allow their curvature radiation to add coherently. Fuller discussion of these other theories is to be found in Manchester and Taylor's book (1977, pp. 205-220).

The positron beam arising from pair production enters the magnetosphere above the gap, still moving along curved magnetic field lines and emitting curvature radiation. The production of pairs as a result of this radiation still occurs as before, but since in the magnetosphere $\bar{E}\cdot\bar{B} = 0$, the pairs do not experience acceleration.

The system of an energetic positron beam moving through a plasma consisting of pair-produced electrons and positrons is prone to the development of plasma waves by the two-stream instability. Cheng and Ruderman (1977a) have shown that the electron-positron plasma must stream

with a velocity difference of $(v_+ - v_-)/c \simeq \pm 10^{-4}$ in order to maintain the charge density of a force-free atmosphere. They find that the instability which develops due to this relative streaming then has a (laboratory) frequency

$$\text{Re } \omega \simeq 3 \times 10^{13} P^{-\frac{1}{2}} B_{12} \left(\frac{a}{r}\right)^{3/2} \quad s^{-1} \qquad (5\text{-}1)$$

and growth rate

$$\text{Im } \omega \simeq 3 \times 10^{8} P^{-\frac{1}{2}} B_{12} \left(\frac{a}{r}\right)^{3/2} \quad s^{-1} \qquad (5\text{-}2)$$

This growth rate is much faster than that associated with the two-stream instability due to the energetic positron beam moving through the plasma (Ruderman and Sutherland 1975), so that bunching will be caused by electron-positron streaming. This is due to the fact that the electron-positron density is a factor $\frac{\gamma_{max}}{2\gamma_{\pm}} \left(\frac{a}{r}\right)^3 > 50$ more than that of the primary beam, due to the large number of curvature-radiation photons produced by the main beam of Lorentz factor γ_{max}, each of which produces pairs with $\gamma_{\pm} = \frac{h\omega}{2mc^2}$. The fact that the plasma wave instability produces bunching is due to the longitudinal nature of $\bar{E}$ in such a wave (Jackson 1975, p. 492). This bunching by separation due to $\bar{E}$ also helps prevent annihilations from occurring. The bunch size will be roughly $2\pi c\omega^{-1}$, where ω is the frequency from (5-1). This size is of the order of centimetres so that coherent radiation will be produced for wavelengths similar to this. Since the spectrum of curvature radiation rises slowly as $(\omega/\omega_c)^{1/3}$ up to the critical frequency ω_c, but falls off exponentially above ω_c (Jackson 1975, pp. 676-677), it is when ω of equation (5-1) is less than or about equal to ω_c that there will be significant radiation

enhancement by coherence (the exponential fall-off of the spectrum overwhelms the coherence increase, which is only a power law with index less than 2 (see e.g. Jackson 1975, p. 514)). The regions where this enhanced emission occurs are delineated in Figure 12. Due to the dependence on r of equation (5-1) the frequency of maximum emission decreases with radius.

At a given frequency (or radius) the emission, essentially tangent to the field lines, occurs between angles θ_{min} and θ_{max}, which are, in degrees (Manchester and Taylor 1977, p. 223)

$$\theta_{min} \simeq 16P^{0.9}\ \omega_{10}{}^{1/3}$$

$$\theta_{max} \simeq 16P^{-0.7}\ \omega_{10}{}^{1/3} \qquad (5\text{-}3)$$

where ω_{10} is the radiation frequency in units of 10^{10} s^{-1}. In a model where the beam is on an oblique rotator (subject to limitations and distortions discussed in Chapter 4) the sweep through the line of sight will determine the pulse shape (Figure 12b). The observed variation of pulse width with period seems to basically agree with (5-3) although the frequency variation does not very well (Manchester and Taylor 1977, p. 223). Spectra and polarization of the pulses are also predicted by this model and are in basic but not very precise accord with observation (Ruderman and Sutherland 1975).

In Chapter 4 the expected .511 MeV annihilation radiation due to positrons (the primary beam) escaping to the interstellar medium was discussed. We have shown that the electron-positron density in the magnetosphere above the polar caps is a factor $\frac{\gamma_{max}}{2\pi_{\pm}} \left(\frac{a}{r^3}\right) \gtrsim 50$ greater

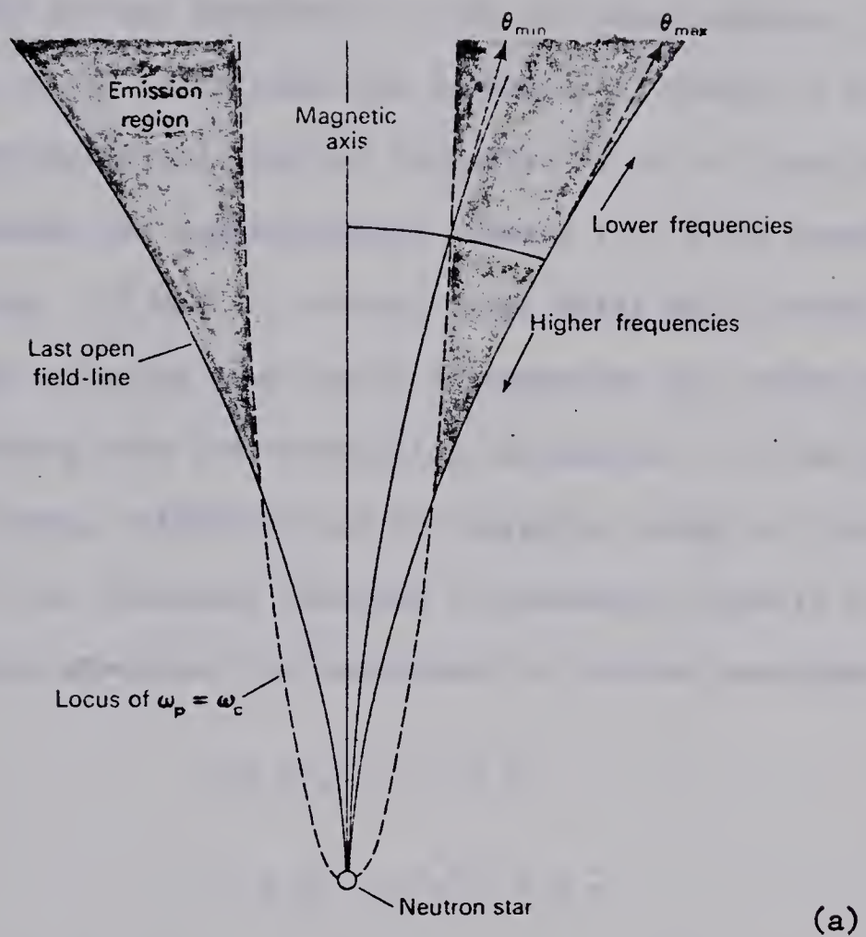

Figure 12. (a) Coherent emission regions above a polar cap (shaded). (from Manchester and Taylor 1977, p. 222)

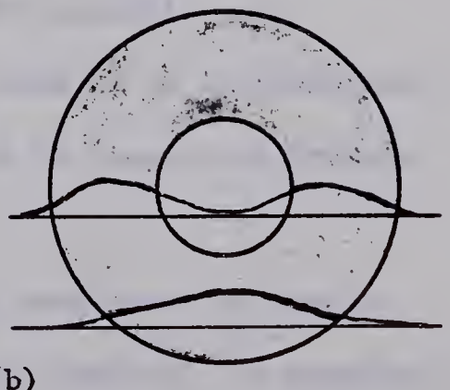

(b) Dependence of pulse shape on sweep of the beam across line of sight.

than that of the primary beam, so what amount of γ-radiation would be expected from this region? Firstly, it should be noted that even if the annihilation photons completely escape the magnetosphere, the resulting flux of say fifty times the estimates of Chapter 4 would still be below current detection limits. Secondly, it is not clear that the photons will escape the magnetosphere. Hardee (1977) has shown that photons of energy .511 MeV (or several times this) should have a mean free path length allowing them easily to penetrate the entire magnetosphere, considering only pair-production attenuation. In the highly relativistic plasma, collisions may be energetic enough to involve pair annihilation to two neutrinos (instead of producing γ-rays), or γ-ray interactions with electrons (or positrons) to produce neutrinos:

$$\begin{aligned} e^+ + e^- &\rightarrow \nu + \bar{\nu} \\ \gamma + e^{\pm} &\rightarrow e^{\pm} + \nu + \bar{\nu} \end{aligned} \qquad (5\text{-}5)$$

(Chiu 1972). Other scattering processes may also be present to prevent .511 MeV line radiation from the magnetosphere, but have not been discussed in the literature in this context. The possible pair annihilation radiation from the magnetosphere leads us to conclude that the photon fluxes calculated in Chapter 4 should be considered minimum, rather than maximum, estimates.

The pair-production discharge theory has been shown to lead to pulsar radiation characteristics similar to those observed, in addition to being consistent with the structure of the overall inner magnetosphere and with ion retention. The ability to consistently describe a number of characteristics of pulsars indicates that future progress

probably depends on improving the understanding of certain details of this theory.

BIBLIOGRAPHY

Anderson, P. W., and N. Itoh, 1975, "Pulsar Glitches and Restlessness as a Hard Superfluidity Problem", Nature 256:25

Andrew, B. H., N. J. B. A. Branson, and D. Willis, 1964, "Radio Observations of the Crab Nebula during a Lunar Occultation", Nature 203:171-173

Angel, J. R. P., 1978, "Magnetic White Dwarfs", Ann. Rev. Astron. Astrophys. 16:487-519

Apparao, K. M. V., 1973, "The Crab Nebula" (Astrophysics and Space Science Review Article), Astrophys. Space Sci. 25:3-116

Apparao, K. M. V., and S. M. Chitre, 1970, "Solar Cycle Theory of Pulsars", Proc. Indian Acad. Sci., Ser. A, Vol. 72, pp. 285-291

Ardavan, H., 1976, "Magnetospheric Shock Discontinuities in Pulsars. I. Analysis of the Inertial Effects at the Light Cylinder", Astrophys. J. 203:226-232

Backus, G., 19 , "The External Field of a Rotating Magnet", Astrophys. J. 123:508-512

Barkat, Z., J. C. Wheeler, and J.-R. Buchler, 1972, "The Evolution of Growing Stellar Cores up to Carbon Ignition: From Whence the Pulsars?" Astrophys. J. 171:651-662

Baym, G., 1974, Lectures on Quantum Mechanics, Benjamin, Reading, Mass.

Baym, G., and C. Pethick, 1975, "Neutron Stars", Ann. Rev. Nucl. Sci. 25:27-77

Blumenthal, G. R., and W. H. Tucker, 1974, "Compact X-Ray Sources", Ann. Rev. Astron. Astrophys. 12:23-46

Bodenheimer, P., and J. P. Ostriker, 1974, "Do Pulsars Make Supernovae? II. Calculations of Light Curves for Type II Events", Astrophys. J. 191:465-471

Börner, G., 1973, "On the Properties of Matter in Neutron Stars", Springer Tracts in Modern Physics (Ergebnisse der Exacten Naturwissenschaften) 69:1-67

Brecher, K., and G. Caporaso, 1977, "'Neutron' Stars Within the Laws of Physics," N.Y.A.S. 302:471-481

Brooks, R. L., 1974, Physics 663 Term Paper, University of Alberta.

Bruenn, S., 1973, "The Carbon Detonation Supernova and Associated Remnant Formation", pp. 213-228 in Schramm and Arnett, 1973

Buckley, R., 1976, "Some Limitations on the Force-Free Approximation to the Physics of Pulsar Magnetospheres", M.N.R.A.S. 177:415-427

Buccheri, R., K. Bennet, G. F. Bignami, N. D'Amico, W. Hermsen, D. J. H. Huizing, G. Kanbach, G. G. Lichti, J. L. Mansou, H. A. Mayer-Hasselwander, J. A. Paul, B. Sacco, B. N. Swanenburg, and R. D. Willis, 1979, Astron. Astrophys.: in press

Burnell, J. Bell, 1977, "Petit Four" (After-Dinner Speech), A.N.Y.A.S. 302:685-689

Buschauer, R., and G. Benford, 1978, "Physical Mechanism of the Goldreich-Keely Radiative Instability", M.N.R.A.S. 185:493-506

Cameron, A. G. W., 1969, "How Are Neutron Stars Formed?" Comments Astrophys. Space Phys. 1:172-177

Canuto, V., 1975a, "Equation of State at High Densities", Ann. Rev. Astron. Astrophys. 13:335-380

Canuto, V., 1975b, "Quantum Processes in Strong Magnetic Fields", A.N.Y.A.S. 257:108-126

Canuto, V., 1975c, "Neutron Stars", pp. 448-527 in Giacconi and Ruffini, 1978

Canuto, V., 1977, "Neutron Stars: General Review", A.N.Y.A.S. 302: 514-527

Chandrasekhar, S., 1956, "Axisymmetric Magnetic Fields and Fluid Motions", Astrophys. J. 124:232-243

Chanmugam, G., 1978, "Stability of Force-Free Magnetic Fields in Degenerate Stars", Astrophys. J. 221:965-968

Chen, H.-H., M. A. Ruderman, and P. G. Sutherland, 1974, "Structure of Solid Iron in Superstrong Neutron-Star Magnetic Fields", Astrophys. J. 191:473-477

Cheng, A. F., and M. A. Ruderman, 1977a, "Bunching Mechanism for Coherent Curvature Radiation in Pulsar Magnetospheres", Astrophys. J. 212:800-806

Cheng, A. F., and M. A. Ruderman, 1977b, "Pair-Production Discharges Above Pulsar Polar Caps", Astrophys. J. 214:598-606

Cheng, A. F., and M. Ruderman, 1977c, "A Crab Pulsar Model: X-Ray, Optical, and Radio Emission", Astrophys. J. 216:865-872

Cheng, A., M. A. Ruderman, and P. Sutherland, 1976, "Current Flow in Pulsar Magnetospheres", Astrophys. J. 203:209-212

Chester, T. J., 1979, "Continuum Optical Pulsation from the Companions of Binary X-Ray Pulsars", Astrophys. J. 227:569-578

Chiu, H. Y., 1972, "A Review of Theories of Pulsars", P.A.S.P. 82: 487-532, reprinted as pp. 351-396 in Chiu and Muriel, 1972

Chiu, H. Y., and V. Canuto, 1971, "Theory of Radiation Mechanisms of Pulsars. I, Astrophys. J. 163:577-594

Chiu, H. Y., and A. Muriel, 1972, Stellar Evolution, M.I.T. Press, Cambridge, Mass.

Chiuderi, C., and H. J. Lee, 1975, "The LOFER (Landau Orbital Ferromagnetism) Mechanism for the Generation of Intense Magnetic Fields", A.N.Y.A.S. 257:82-84

Clark, D. H., and J. L. Caswell, 1976, "A Study of Galactic Supernova Remnants, Based on Molonglo-Parkes Observational Data", M.N.R.A.S. 174:267

Cohen, J. M., and A. Rosenblum, 1972, "Pulsar Magnetosphere", Ap. Space Sci. 16:130

Cohen, J. M., and E. T. Toton, 1971, "Pulsar Electrodynamics", Astrophys. Letters 7:213-215

Cohen, R., J. Logenquai, and M. Ruderman, 1970, "Atoms in Superstrong Magnetic Fields", Phys. Rev. Letters 25:467-469

Coles, W. A., and J. J. Kaufmann, 1977, "Angular Size of the Crab Pulsar at 74 MHz", M.N.R.A.S. 181:57P-59P

Constantinescu, D. H., and P. Rehák, 1973, "Ground State of Atoms and Molecules in a Superstrong Magnetic Field", Phys. Rev. D 8: 1693-1706

Contopoulos, G. (ed.), 1974, Highlights of Astronomy, Volume 3, D. Reidel, Dordrecht, Holland

Cordes, J. M., 1975, "Pulsar Microstructure: Time Scales, Spectra, Polarization, and Radiation Models", Thesis, University of California at San Diego, cited in Manchester and Taylor, 1977

Cowling, T. G., 1976, Magnetohydrodynamics, Adam Hilger, Ltd., Bristol, England

Damashek, M., and J. H. Taylor, 1978, "Parameters of 17 Newly Discovered Pulsars in the Northern Sky", Astrophys. J. Lett. Ed. 225:L31-33

Davidson, P. J. N., M. G. Watson, and J. P. Pye, 1977, "The Binary X-Ray Pulsar 3U 1538-52", M.N.R.A.S. 181:73P-79P

Davies, R. D., and F. G. Smith, 1971, The Crab Nebula (I.A.U. Symposium No. 46), Springer, New York

Davis, L., Jr., 1948, "Stellar Electromagnetic Fields", Phys. Rev. 72: 632-633

Deutsch, A. J., 1955, "The Electromagnetic Field of an Idealized Star in Rigid Rotation in Vacuo", Ann. d'Ap. 18:1

Drake, F. D., "Radio Observations of the Crab Nebula Pulsar", pp. 73-83 in Davies and Smith, 1971

Durney, B. R., J. Faulkner, J. R. Gribbin, and I. W. Roxburgh, 1968, "Pulsation Periods of Rotating White Dwarfs", Nature 219:20-21, reprinted as pp. 55-56 of Smith and Hewish, 1968

Erber, T., 1966, "High-Energy Electromagnetic Conversion Processes in Intense Magnetic Fields", Rev. Mod. Phys. 38:626-659

Ewart, G. M., R. A. Guyer, and G. Greenstein, 1975, "Electrical Conductivity and Magnetic Field Decay in Neutron Stars", Astrophys. J. 202:238-247

Fawley, W. M., J. Arons, and E. T. Scharlemann, 1977, "Potential Drops Above Pulsar Polar Caps: Acceleration of Nonneutral Beams from the Stellar Surface", Astrophys. J. 217:227-243

Ferrari, A., and E. Trussoni, 1973, "Magnetic Fields Around Highly Magnetized Objects", Astrophys. Space Sci. 24:3-15

Ferrari, A., and E. Trussoni, 1974, "Acceleration by Oblique Magnetic Rotators: Near Fields and Radiation Braking", Astron. Astrophys. 36:267-272

Flowers, E., and M. A. Ruderman, 1977, "Evolution of Pulsar Magnetic Fields", Astrophys. J. 215:302-310

Flowers, E. G., J.-F. Lee, M. A. Ruderman, P. G. Sutherland, W. Hillebrandt, and E. Müller, 1977, "Variational Calculation of Ground-Condensed Matter in Strong Magnetic Fields", Astrophys. J. 215, 291-301

von Foerster, T., 1979, "Gravity Waves Slow Binary Pulsar", Physics Today 32(5):19-20

Frauenfelder, H., and E. M. Henley, 19 , Subatomic Physics, Prentice-Hall, Englewood Cliffs, N.J.

Gailly, J. L., J. Lequeux, and J. L. Mansou, 1978, "The z-distribution and Birthrate of Pulsars from the New Molonglo Survey", Astron. Astrophys. 70:L15-L18

Ghosh, P., F. K. Lamb, and C. J. Pethick, 1977, "Accretion by Rotating Magnetic Neutron Stars. I. Flow of Matter Inside the Magnetosphere and its Implications for Spin-Up and Spin-Down of the Star", Astrophys. J. 217:578-596

Giacconi, P., and R. Ruffini, 1978, "Physics and Astrophysics of Neutron Stars and Black Holes", Proceedings of the International School of Physics "Enrico Fermi" (July 1975), North-Holland, New York

Ginzburg, V. L., and V. V. Zheleznyakov, 1975, "On the Pulsar Emission Mechanism", Ann. Rev. Astron. Astrophys. 13:511-535

Gold, T., 1968, "Rotating Neutron Stars as the Origin of the Pulsating Radio Sources", Nature 218:731-732, reprinted in Smith and Hewish 1968, pp. 74-75, and in Gursky and Ruffini 1975, pp. 354-356

Gold, T., 1969, Pulsating Stars 2 (a Nature Reprint), Macmillan, London

Goldreich, P., and W. H. Julian, 1969, "Pulsar Electrodynamics", Astrophys. J. 157:869-880

Goldreich, P., F. Pacini, and M. Rees, 1971, "Pulsar Theory I. Dynamics and Electrodynamics", Comments Astrophys. Space Phys. 3: 185-189

Goldreich, P., F. Pacini, and M. Rees, 1972, "Pulsar Theory II. Radiation Mechanisms", Comments Astrophys. Space Phys. 4:23-28

Gomer, R., 1961, Field Emission and Field Ionization, Harvard U. Press, Cambridge, Mass.

Gopal-Krishna, 1978, "A Ghost Supernova Remnant Around PSR0950+08", M.N.R.A.S. 185:521-525

Groth, E. J., 1972, "Crab Timing Observations", A.N.Y.A.S. 224: 184-189

Groth, E. J., 1975, "Timing of the Crab Pulsar. I. Arrival Times", Astrophys. J. Suppl. Ser. 29:431-442

Gullahorn, G., and J. M. Rankin, 1978a, "Pulsar Proper Motions from Timing Observations", Astrophys. J. 225:963-969

Gullahorn, G., and J. M. Rankin, 1978b, "Pulsar Timing Results from Arecibo Observatory", Astronom. J. 83:1219-1224

Gunn, J. E., and J. P. Ostriker, 1970, "On the Nature of Pulsars III. Analysis of Observations", Astrophys. J. 160:979-1002

Gunn, J. E., and J. P. Ostriker, 1971, "On the Motion and Radiation of Charged Particles in Strong Electromagnetic Waves. I. Motion in Plane and Spherical Waves", Astrophys. J. 165:523-541

Gursky, H., and R. Ruffini, 1975, Neutron Stars, Black Holes and Binary X-Ray Sources, Reidel, Dordrecht, Holland

Haines, L. K., and D. H. Roberts, 1969, "One-Dimensional Hydrogen Atom", Amer. J. Phys. 37:1145-1154

Hansen, C. J., 1974, Physics of Dense Matter, I.A.U. Symposium No. 53, Reidel, Dordrecht, Holland

Hardee, P. E., 1977, "Production and Beaming of Pulsar γ-Ray Emission", Astrophys. J. 216:873-880

Harrison, E. R., 1970, "Bouncing-Core Theory of Pulsars", Nature 225: 44-46

Hewish, A., S. J. Bell, J. D. H. Pilkington, P. F. Scott, and R. A. Collins, 1968, "Observation of a Rapidly Pulsating Radio Source", Nature 217:709-713, reprinted in Smith and Hewish 1968, pp. 5-9, and in Sursky and Ruffini 1975, pp. 344-353

Hillebrandt, W., and E. Müller, 1976, "Matter in Superstrong Magnetic Fields and the Structure of a Neutron Star's Surface", Astrophys. J. 207:589-591

Hinata, S., 1978, "Stability of Force-Free Pulsar Wind Zone", Astrophys. J. 221:1003-1008

Hinata, S., 1979, "Inhomogeneous Pulsar Polar Cap Structure and Radiation Processes", Astrophys. J. 227:275-284

Hinata, S., and E. A. Jackson, 1974, "On the Axisymmetric Pulsar Atmosphere", Astrophys. J. 192:703-711

Holloway, N. J., 1973, "p-n Junctions in Pulsar Magnetospheres?" Nature Phys. Sci. 246:6-9

Hones, E. W., and J. E. Bergeson, 1965, "Electric Field Generated by a Rotating Magnetized Sphere", J. Geophys. Res. 70:4951-4958

Hoyle, F., and J. Narlikar, 1968, "Pulsed Radio Sources", Nature 218: 123-124, reprinted as pp. 51-52 in Smith and Hewish 1968

Huang, K., 1963, Statistical Mechanics, Wiley, New York

Huguenin, G. R., J. H. Taylor, R. M. Hjellming, and C. M. Wade, 1971, "Interferometric Observations of Pulsars at 2.7 and 8.1 GHz", Nature 234:50-51

Ilovaisky, S. A., Ch. Motch, and C. Chevalier, 1978, "Discovery of Optical Pulsations from 4U1626-67", Astron. Astrophys. 70:L19-L22

Israel, W., 1968a, "Model for Pulsed Radio Sources", Nature 218: 755-756, reprinted as pp. 61-62 in Smith and Hewish 1968

Israel, W., 1968b, "Pulsar Condition in White Dwarf Stars", Nature 218: 1235-1236, reprinted as pp. 63-64 in Smith and Hewish 1968

Israel, W., 1974, Physics 663 Lecture Notes, University of Alberta

Jackson, E. A., 1976a, "Pulsar Atmospheric Current Loops", Nature 259: 25-26

Jackson, E. A., 1976b, "A New Pulsar Atmospheric Model I. Aligned Magnetic and Rotational Axes", Astrophys. J. 206:831-841

Jackson, E. A., 1978a, "Responses to Perturbations of the Force-Free Aligned Pulsar Atmosphere", M.N.R.A.S. 183:445-457

Jackson, E. A., 1978b, "Theory of the Pulsar Atmosphere II: Arbitrary Magnetic and Rotational Axes; Qualitative Features", Astrophys. J. 222:675-688

Jackson, E. A., 1979, "Minimum Energy State of the Constrained Pulsar Atmosphere", Astrophys. J. 227:266-274

Jackson, J. D., 1975, Classical Electrodynamics, Second Edition, Wiley, New York

Jenkins, R. O., and W. G. Trodden, 1965, Electron and Ion Emission from Solids, Routledge and Keegan Paul, London

Kadomtsev, B. B., 1970, "Heavy Atom in an Ultrastrong Magnetic Field", Zh. Eksp. Teor. Fiz. 58:1765-1769, rep. Soviet Physics JETP 31: 945-947

Kadomtsev, B. B., and V. S. Kudryatsev, 1971a, "Molecules in a Superstrong Magnetic Field", Zh. Eksp. Teor. Fiz. Pis. Red. 13:15-19, rep. Soviet Physics JETP Lett. 13:9-12

Kadomtsev, B. B., and V. S. Kudryatsev, 1971b, "Atoms in a Superstrong Magnetic Field", Zh. Eksp. Teor. Fiz. Pis. Red. 13:61-64, rep. Soviet Physics JETP Lett. 13:42-44

Karpman, V. I., C. A. Norman, D. ter Haar, and V. N. Tsytovich, 1975, "Relativistic Solitons and Pulsars", Physica Scripta 11:271-274

Kristian, J., 1970, "On the Optical Identification of the Vela Pulsar: Photoelectric Measurements", Astrophys. J. (Lett.) 162:L103-L104

Kuo-Petravic, L. G., M. Petravic, and K. V. Roberts, 1974, "Self-Consistent Solution for an Axisymmetric Pulsar Model", Phys. Rev. Lett. 32:1019-1022

Kuo-Petravic, L. G., and M. Petravic, 1976, "Comment on 'Self-Consistent Solution for an Axisymmetric Pulsar Model'", Phys. Rev. Lett. 36:686-688

Kuo-Petravic, L. G., M. Petravic, and K. V. Roberts, 1976, "Numerical Studies of the Axisymmetric Pulsar Magnetosphere", Astrophys. J. 202:762-772

Lamb, F. K., 1977, "Knowledge of Neutron Stars from X-Ray Observations", A.N.Y.A.S. 302:482-513

Landau, L. D., 1932, "On the Theory of Stars", Phys. Z. Sowjetunion 1:285, reprinted in: Lifshitz, E. M., and Chalatnikova, I. M., as "K teorii zvyozd" 1969, and as pp. 271-273 in Gursky and Ruffini 1975

Landau, L. D., and E. M. Lifshitz, 1962, The Classical Theory of Fields, Addison-Wesley, Reading, Mass.

Landau, L. D., and Lifshitz, E. M., 1977, Quantum Mechanics (Non-Relativistic Theory), Third Edition, Pergamon, Oxford

Lenchek, A. M. (ed.), 1972, The Physics of Pulsars, Gordon and Breach, New York

Leventhal, M., J. C. MacCallum, and A. C. Watts, 1977a, "A Search for Gamma-Ray Lines from Nova Cygni 1975, Nova Serpentis 1970, and the Crab Nebula", Astrophys. J. 216:491-502

Leventhal, M., J. C. MacCallum, and A. C. Watts, 1977b, "Possible Gamma-Ray Line from the Crab Nebula", A.N.Y.A.S. 302:532-537

Levi, B. G., 1977, "Evidence for 10^{12}-Gauss Field on Neutron Star", Physics Today 30(6):19-20

Lifshitz, E. M., and I. M. Chalatnikova, 1969, L. D. Landau - Sobranije Trudov, Nauka, Moscow

Lingenfelter, R. E., and R. Ramaty, 1978, "Gamma-Ray Lines: A New Window to the Universe", Physics Today 31(3):40-48

Lodenquai, J., V. Canuto, M. Ruderman, and S. Tsuruta, 1974, "Photon Opacity in Surfaces of Neutron Stars", Astrophys. J. 190:141-152

Lorrain, P., and D. Corson, 1970, Electromagnetic Fields and Waves, Freeman, San Francisco

Lyne, A. G., 1977, "A New Pulsar Survey", Proc. Astron. Soc. Aust. 3: 118-120

Manchester, R. N., 1979, Pulsars, CSIRO Preprint RPP 2283

Manchester, R. N., and J. H. Taylor, 1977, Pulsars, Freeman, San Francisco

Manchester, R. N., A. G. Lyne, J. H. Taylor, J. M. Durdin, M. I. Large, and A. G. Little, 1978, "The Second Molonglo Pulsar Survey - Discovery of 155 Pulsars", M.N.R.A.S. 185:409-421

Mathews, J., and R. L. Walker, 1970, Mathematical Methods of Physics, Benjamin, Menlo Park, California

Mertz, L., 1974, "Mode-Locked Maser Theory of Pulsars", Astrophys. Space Sci. 30:43-55

Mestel, L., 1961, "A Note on Equatorial Acceleration in a Magnetic Star", Astrophys. J. 122:473-478

Mestel, L., 1968, "Magnetic Braking by a Stellar Wind - I, M.N.R.A.S. 138:359-391

Mestel, L., 1971, "Pulsar Magnetosphere", Nature Phys. Sci. 233, 149-152

Mestel, L., 1973, "Force-Free Pulsar Magnetospheres", Astrophys. Space Sci. 24:289-298

Michel, F. C., 1969, "Relativistic Stellar-Wind Torques", Astrophys. J. 158:727-738

Michel, F. C., 1973a, "Rotating Magnetosphere: A Simple Relativistic Model", Astrophys. J. 180:207-225

Michel, F. C., 1973b, "Rotating Magnetospheres: An Exact 3-D Solution", Astrophys. J. Lett. 180:L133-L137

Michel, F. C., 1974, "Rotating Magnetosphere: Acceleration of Plasma from the Surface", Astrophys. J. 192:713-718

Michel, F. C., 1975a, "Rotating Magnetospheres: Frozen-in-Flux Violation", Astrophys. J. 196:579-582

Michel, F. C., 1975b, "Self-Consistent Rotating Magnetosphere", Astrophys. J. 197:193-197

Michel, F. C., 1975c, "Composition of the Neutron Star Surface in Pulsar Models", Astrophys. J. 198:683-685

Michel, F. C., 1978a, "A Phenomenological Pulsar Model", Astrophys. J. 220:1101-1106

Michel, F. C., 1978b, "Fundamental Pulsar Luminosity", Astrophys. J. 224:988-992

Michel, F. C., 1979, "Vacuum Gaps in Pulsar Magnetospheres", Astrophys. J. 227:579-589

Miller, J. S., and E. J. Wampler, 1969, "Television Detection of the Crab Nebula Pulsar", Nature 221:1037-1038

Mitton, S., 1979, The Crab Nebula, Faber and Faber, London

Morris, D., V. Radhakrishnan, and C. S. Shukre, 19 , "Three Proposed Pulsar/Supernova Remnant Associations and Their Possible Origin in Close Binary Systems", Astron. Astrophys. 68:289-293

Morrison, P., 1969, "Are Quasi-Stellar Radio Sources Giant Pulsars?" Astrophys. J. (Lett.) 157:L73-L76

Morse, P. M., and H. Feshbach, 1953, Methods of Theoretical Physics (Part I), McGraw-Hill, New York

Mueller, R. O., A. R. P. Rau, and L. Spruch, 1971, "Magnetic Field Effects on the Outermost Crusts of Pulsars", Nature Phys. Sci. 234: 31-32

Nather, R. E., E. L. Robinson, G. W. Van Citters, P. D. Hemenway, 1977, "An Upper Limit to Optical Pulses from the Binary Pulsar PSR1913+16", Astrophys. J. Lett. 211:L125-L127

Occhionero, F., and M. Demianski, 1969, "Electric Fields in Rotating, Magnetic, Relativistic Stars", Phys. Rev. Lett. 23:1128-1130

Ögelman, H., C. E. Fichtel, D. A. Kniffen, and D. J. Thompson, 1976, "A Search of the SAS-2 Data for Pulsed Gamma-Ray Emission from Radio Pulsars", Astrophys. J. 209:584

Okamoto, I., 1974, "Force-Free Pulsar Magnetosphere - I, M.N.R.A.S. 167:457-474

Okamoto, I., 1975, "Force-Free Pulsar Magnetosphere - II, M.N.R.A.S. 170:81-93

Ostriker, J. P., 1968, "Possible Model for a Rapidly Pulsating Radio Source", Nature 217:1127-1128, reprinted as pp. 73-74 in Smith and Hewish 1978

Ostriker, J. P., 1972, "Pulsars and the Origin of Cosmic Rays", pp. 159-170 in Lenchek 1972

Ostriker, J. P., and J. E. Gunn, 1969, "On the Nature of Pulsars I: Theory", Astrophys. J. 157:1395-1417

Pacholczyk, A. G., 1970, Radio Astrophysics, Freeman, San Francisco

Pacini, F., 1967, "Energy Emission from a Neutron Star", Nature 215: 567-568

Pacini, F., 1971, "The Secular Decrease of the Optical and X-Ray Luminosity of Pulsars", Astrophys. J. Lett. 163:L17-L19

Pacini, F., 1973, "Pulsar Electrodynamics", A.N.Y.A.S. 224:135-143

Pacini, F., and M. J. Rees, 1970, "The Nature of Pulsar Radiation", Nature 226:622-624

Parrish, J. L., 1974, "Pulsar Near Fields", Astrophys. J. 193:225-229

Peterson, B. A., P. Murdin, P. Wallace, R. N. Manchester, A. J. Penny, A. Jorden, K. F. Hartley, and D. King, 1978, "Pulsed and Unpulsed Light from the Vela and Crab Pulsars", Nature 276:475-478

Petravic, M., 1976, "Numerical Modelling of Pulsar Magnetospheres", Comp. Phys. Comm. 12:9-19

Pines, D., J. Shaham, and M. A. Ruderman, 1974, "Neutron Star Structure from Pulsar Observations", pp. 189-207 in Hansen 1974 (also published in A.N.Y.A.S. 224:190-205)

Press, W. H., and K. S. Thorne, 1972, "Gravitational-Wave Astronomy", Ann. Rev. Astron. Astrophys. 10:335-374

Rabi, I. I., 1928, "Das freie Elektron im homogenen Magnetfeld nach der Diracschen Theorie", Zs. f. Physik 49:507-511

Ramaty, R., G. Borner, and J. M. Cohen, 1973, "Positron-Annihilation Radiation from Neutron Stars", Astrophys. J. 181:891-894

Ramaty, R., and R. E. Lingenfelter, 1979, "γ-Ray Line Astronomy", Nature 278:127-132

Rao, A. P., and S. Krishnamohan, 1972, "Accurate Position of PSR1749-28 from Lunar Occultations", Nature Phys. Sci. 238:69

Rappaport, S., and P. C. Joss, 1977a, "Binary X-Ray Pulsars", Nature 266:123-125

Rappaport, S., and P. C. Joss, 1977b, "The Masses of Neutron Stars: Observational Constraints", A.N.Y.A.S. 302:460-470

Richards, D. W., and J. M. Comella, 1969, "The Period of Pulsar NP0532", Nature 222:551-552, reprinted on pp. 17-18 of Gold 1969

Roberts, D. H., P. A. Sturrock, and J. S. Turk, 1973, "Magnetosphere Structure and Radiation Mechanism of Pulsars", A.N.Y.A.S. 224: 206-217

Roberts, W. J., 1979, "Electromagnetic Multipole Fields of Neutron Stars", Astrophys. J., in press

Routledge, D., 1979, Electrical Engineering 602 Lecture Notes, University of Alberta

Ruderman, M. A., 1971, "Matter in Superstrong Magnetic Fields: The Surface of a Neutron Star", Phys. Rev. Lett. 27:1306-1308

Ruderman, M., 1972, "Pulsars: Structure and Dynamics", Ann. Rev. Astron. Astrophys. 10:427-476

Ruderman, M., 1974, "Matter in Superstrong Magnetic Fields", pp. 117-131 in Hansen 1974

Ruderman, M., 1975, "Matter and Magnetospheres in Superstrong Magnetic Fields", A.N.Y.A.S. 257:127-140

Ruderman, M. A., 1976a, "Crust-Breaking by Neutron Superfluids and the Vela Pulsar Glitches", Astrophys. J. 203:213-222

Ruderman, M. A., 1976b, "Direction of Subpulse Drifting Within Pulsar Radio Emission Envelopes", Astrophys. J. 203:206-208

Ruderman, M., and P. Sutherland, 1975, "Theory of Pulsars: Polar Gaps, Sparks, and Coherent Microwave Radiation", Astrophys. J. 196:51-72

Saenz, R. A., 1977, "Maximum Mass of Neutron Stars: Dependence on the Assumptions", Astrophys. J. 212:816-824

Saslaw, W. C., J. Faulkner, and P. A. Strittmayer, 1968, "Rapidly Pulsing Radio Sources", Nature 217:1322-1326, reprinted as pp. 78-82 in Smith and Hewish 1968

Scargle, J. D., and F. Pacini, 1971, "On the Mechanism of the Glitches in the Crab Nebula Pulsar", Nature Phys. Sci. 232:144-149

Scharlemann, E. T., 1974, "Aligned Rotating Magnetospheres II. Inclusion of Inertial Forces", Astrophys. J. 193:217-223

Scharlemann, E. T., 1977, "The Fate of Matter and Angular Momentum in Disk Accretion Onto a Magnetized Neutron Star", Astrophys. J. 219: 617-628

Scharlemann, E. T., J. Arons, and W. M. Fawley, 1978, "Potential Drops Above Pulsar Polar Caps: Ultrarelativistic Particle Acceleration Along the Curved Magnetic Field", Astrophys. J. 222: 297-316

Scharlemann, E. T., and R. V. Wagoner, 1973, "Aligned Rotating Magnetospheres I. General Analysis", Astrophys. J. 182:951-960

Scheuer, P. A. G., 1962, "On the Use of Lunar Occultations for Investigating the Angular Structure of Radio Sources", Aust. J. Phys. 15:333-343

Schiff, L. I., 1939, "A Question of General Relativity", Proc. Nat. Acad. Sci. 25:391-395

Schmidt, G. D., J. R. P. Angel, and E. A. Beaver, 1979, "The Small-Scale Polarization of the Crab Nebula", Ap. J. 227:106-113

Schramm, P. N., and W. D. Arnett, 1973, Explosive Nucleosynthesis, University of Texas, Austin

Shapiro, S. L., and Y. Terzian, 1976, "Galactic Rotation and the Binary Pulsar", Astron. Astrophys. 52:115-118

Smith, R. G. (ed.), 1974, "Jovian Radio Bursts and Pulsars", pp. 493-498 in Contopoulos 1974

Smith, F. G., 1977, Pulsars, Cambridge University Press, Cambridge, England

Smith, F. G., and A. Hewish, 1968, Pulsating Stars (a Nature Reprint), Macmillan, London

Sturrock, P. A., 1971, "A Model of Pulsars", Astrophys. J. 164: 529-556

Sturrock, P. A., V. Petrosian, and J. S. Turk, 1975, "Optical Radiation from the Crab Pulsar", Astrophys. J. 196:73-82

Swann, W. F. G., 1920, "Unipolar Induction", Phys. Rev. 15:365-398

Taylor, J. H., L. A. Fowler, and P. M. McCulloch, 1979, "Measurements of General Relativistic Effects in the Binary Pulsar PSR1913+16", Nature 277:437-440

Taylor, J. H., and R. N. Manchester, 1975, "Observed Properties of 147 Pulsars", Astron. J. 80:794-806

Taylor, J. H., and R. N. Manchester, 1977a, "Recent Observations of Pulsars", Ann. Rev. Ast. Ap. 15:19-44

Taylor, J. H., and R. N. Manchester, 1977b, "Galactic Distribution and Evolution of Pulsars", Astrophys. J. 215:885-896

Trümper, J., W. Pietsch, C. Reppin, B. Sacco, E. Kendziorra, and R. Staubert, 1977, "Evidence for Strong Cyclotron Emission in the Hard X-Ray Spectrum of Her X-1", A.N.Y.A.S. 302:538-544

Tsuruta, S., 1974, "Cooling of Dense Stars", pp. 209-225 in Hansen 1974

Tucker, W. H., 1975, Radiation Processes in Astrophysics, MIT Press, Cambridge, Mass.

Van Paradijs, J. A., G. Hammerschlag-Hensberge, E. P. J. van den Heuvel, R. J. Takens, E. J. Zuiderwijk, and C. De Loore, 1976, "Mass Determination for the X-Ray Binary System Vela X-1", Nature 259: 547-549

Wampler, E. J., 1972, "Optical Observations of Pulsars", pp. 21-32 in Lenchek 1972

Wampler, E. J., J. D. Scargle, and J. S. Miller, 1969, "Optical Observations of the Crab Nebula Pulsar", Astrophys. J. (Lett.) 157: L1-L10

Warner, B., R. E. Nather, and M. MacFarlane, 1969, "Further Observations of the Crab Nebula Optical Pulsar", Nature 222:233

Webster, D. L., and R. C. Whitten, 1973, "Which Electromagnetic Equations Apply in Rotating Coordinates?" Astrophys. Space Sci. 24:323-333

Weinberg, S., 1972, Gravitation and Cosmology: Principles and Applications of the General Theory of Relativity, Wiley, New York

Wheeler, J. A., 1966, "Superdense Stars", Ann. Rev. Astron. Astrophys. 4:393-432

Wheeler, J. Craig, 1973, "The Carbon Detonation Supernova Model", pp. 203-212 in Schramm and Arnett 1973

Wichman, E., 1971, Quantum Physics, McGraw-Hill, New York

Wildi, T., 1972, Units, Volta, Sillery, P.Q.

Woltjer, L., 1975, "Astrophysical Evidence for Strong Magnetic Fields", A.N.Y.A.S. 257:76-79

Wright, G. A. E., 1979, "The Possibility of Accretion Onto Radio Pulsars", Nature 280:40-41

APPENDIX 1

Sources of Statistical Data

Manchester and Taylor 1977 (Appendix)

Damashek, Taylor, and Hulse 1978

Manchester et al. 1978

These sources present data for 321 pulsars. Some synthesis of these data in graphical form is given by Manchester (1979).

APPENDIX 2

Characteristic Ages of 20 Pulsars and Braking Indices of 9 Pulsars Based on Recent Timing Results

Pulsar frequencies and derivatives were observed with the Arecibo radio telescope and published by Gullahorn and Rankin (1978b). The frequencies and first derivatives were converted to period and period derivative and are presented as Table A-1, along with the characteristic age in millions of years (Ma). These data are also presented in Figures 5 and 6, where they are seen to blend in with older data without introducing any significant statistical changes to those data. Table A-2 presents frequencies and their first and second derivatives for 10 pulsars - the first nine represent new results, also from the (1978b) paper of Gullahorn and Rankin. The last listing, given for comparison, is the Crab Pulsar, where the derivatives are well known due to their comparatively large magnitude (Groth 1975). The braking indices listed in the last column have been calculated from the data in the table. The fact that they seem unreasonable in sign and magnitude (when compared to the Crab or to theoretical values of about 3) casts considerable doubt on the second derivatives determined by Gullahorn and Rankin. These authors are currently preparing a series of papers discussing these results.

Table A-1. Periods, Period First Derivatives, and Characteristic Ages $T_6 = \frac{1}{2}P/\dot{P}$ for 20 Pulsars, Calculated from Data by Gullahorn and Rankin (1978b).

P	P(s)	$\dot{P}(10^{-15}ss^{-1})$	T_6(Ma)
1900+05	.7465697	12.896013	.917
1906+09	.8302699	.0987758	133.2
1907+12	1.4417376	8.2446963	2.77
1911+13	.5214722	.8052111	10.3
1911+11	.6009975	.6555952	14.5
1913+167	1.6162314	.4076089	62.9
1913+10	.4045304	15.244140	.421
1914+09	.2702529	2.5182870	1.70
1914+13	.2818403	3.6172045	1.235
1916+14	1.1808838	211.35010	.089
1919+14	.6181797	5.6120633	1.75
1924+16	.5798119	18.003483	.511
1924+14	1.3249220	.2232364	94.1
1925+22	1.4310666	.7705831	29.4
1927+13	.7600320	3.6609526	3.29
1929+20	.2682148	4.1853985	1.016
1929+20	.2682149	4.1786406	1.018
1930+22	.1444279	57.779728	.040
1933+15	.9673384	4.0386196	3.798
1944+22	1.3344500	.8886812	23.8
2028+22	.6305121	.3837774	11.3

Table A-2. Frequencies, First and Second Derivatives, and Braking Indices $n = \frac{\nu\ddot{\nu}}{\dot{\nu}^2}$ for 9 Pulsars, Calculated from Data by Gullahorn and Rankin (1978b), and for the Crab Pulsar P0831+21, from Groth (1975).

P	ν (Hz)	$\dot{\nu}(10^{-15}\text{Hz s}^{-1})$	$\ddot{\nu}(10^{-25}\text{Hz s}^{-2})$	n
0540+23	4.0656	-255.022	3.953	24.71
0950+08	3.9516	-3.57820	-1.704	-12664.70
1541+09	1.3361	-.768157	-1.116	-252698.8
1859+03	1.5257	-17.42847	1.100	552.51
1907+00	.983337	-5.332848	-2.490	-8609.61
1915+13	5.13805	-190.1523	-6.440	-91.51
1929+10	4.41468	-22.54446	-3.18	-2762.16
2002+31	.47366046	-16.7302	7.126	1205.93
2020+28	2.912049	-16.08157	1.028	1157.74
0831+21	30.2058647	-3.855969×10^5	1.234084×10^5	2.5071

APPENDIX 3

Very Recent Results

Among the most interesting results communicated at the General Assembly of the I.A.U. in Montreal in August was the discovery, among the Molonglo II pulsars, of a new binary pulsar. In contrast to the short-period P1913+16, the new system, P0820+02 has a period of 1265 d, and $\frac{a \sin i}{c}$ of 171 s (if $\dot{P} = 0$), according to B. J. Robinson, so that the easy observation of relativistic effects is not expected. Nevertheless, the discovery of this system brings the "statistics" of binary radio pulsars (2 among 328 pulsars) back into line with the expectations of binary evolution theory (see Chapter 2 and reference therein). J. H. Taylor announced that the pulse shape changes "observed" in P1913+16 (Taylor et al. 1978) are probably an observational effect. He also advanced the idea that interpulses may not represent emission from two polar caps but simply be an extreme case of wide pulses - a pulse-width histogram supports this hypothesis.

A. G. Lyne presented Jodrell Bank astrometry results on 9 pulsars. P1920+10 is located 69 ± 26 pc away, but for the 8 others studied, the errors are larger than the measurements (the parallax is of order 10^{-3} arcsec and is measured through interferometry with a 127 km baseline). Distances based on dispersion measure are comparable to those of these parallaxes if a value of $\langle Ne \rangle = .03$ cm^{-3} is adopted for the electron density (see also the letter by Salter, Lyne, and Anderson in Nature, vol. 280, pp. 477-478).

The theoretical paper of most relevance to the Ruderman-Sutherland class of models was presented by V. Radhakrishnan. Assuming that pair-production discharges in a polar cap gap are initiated solely by background γ-rays, and noting that the path length (see equation 4-65) is a decreasing function of the photon energy, he finds that the magnetosphere acts as a low-pass filter, on photons. The most energetic of these photons entering the gap will have the most chance of initiating discharges, so that in a given magnetic field a band of photon energies is selected as possible initiators of discharges. Conversely, given the natural background spectrum, one can find that fields of $B_{12} = 1$ to 3 are needed for pair-production. This correlates well with fields determined from $(P\dot{P})^{\frac{1}{2}}$.

A final recent report of major importance is the "Possible optical observation of the companion star to the binary pulsar PSR1913+16" (Nature 280, pp. 367-370), in which P. Crane, J. Nelson, and J. Tyson report observing a star of $M_R = 20.9$ at the precise coordinates of the pulsar. Their interpretation of this object as a helium (i.e., helium-burning main-sequence) star would introduce tidal effects to the binary system which disallow the interpretation (Taylor et al. 1978) of timing effects as due to gravitational radiation. The suggested confirmation (spectroscopically) of this object as a helium star companion to PSR1913+16 is of obvious importance.